LA-UR--85-2730

DE85 015731

TITLE: The Three-Nucleon Problem: Trinucleon Bound States and Trinucleon Interactions

AUTHOR(S): J. L. Friar, T-5

SUBMITTED TO: Lecture to be given at, "New Vistas in Electronuclear Physics," 1985 NATO Advanced Study Institute, Banff, Alberta, Canada, August 22 - September 4, 1985.

THE THREE-NUCLEON PROBLEM:
1) Trinucleon Bound States
2) Trinucleon Interactions

J. L. Friar

Theoretical Division
Los Alamos National Laboratory
Los Alamos, NM 87545 USA

ABSTRACT

The assumptions underlying the formulation and solution of the Schrödinger equation for three nucleons in configuration space are reviewed, in conjunction with those qualitative aspects of the two-nucleon problem which are important. The geometrical features of the problem and the crucial role of the angular momentum barrier are developed. The boundary conditions for scattering are discussed qualitatively, and the Faddeev-Noyes equation is motivated. The method of splines and orthogonal collocation are shown to provide convenient techniques for generating numerical solutions. Properties of the many numerical solutions for the bound states and zero-energy scattering states are discussed. The evidence for three-body forces is reviewed, and the results of the recent calculations including such forces are discussed. The importance of electromagnetic interactions in the three-nucleon systems is motivated. Relativistic corrections and meson-exchange currents are discussed in the context of "rules of scale", and the pion-exchange currents of nonrelativistic order are derived. The experimental results for trinucleon electromagnetic interactions are reviewed, including recent tritium data. Conclusions are presented.

LECTURE 1. TRINUCLEON BOUND STATES

I. INTRODUCTION

The four bound few-nucleon systems (^{2}H, ^{3}H, ^{3}He, ^{4}He) have played a role in nuclear physics far out of proportion to their abundance on earth, and their study constitutes one of the oldest and most important subfields of our discipline. In one of the first review articles[1] treating nuclear physics, a separate section was reserved for the three-nucleon problem. Since that time many such articles have been written.

The special importance of these four nuclei stems from the great difficulty in solving the many-body problem. Special techniques exist for solving that problem when the number of particles becomes huge, a limit of no obvious relevance to nuclear physics. On the other hand we can also solve "exactly" (in the numerical sense) well-posed model problems with four or fewer nucleons. Our lack of ability to construct from first principles a tractable Hamiltonian for the interaction of a single pair of nucleons which describes all the phenomena associated with this system means that we routinely use semiphenomenological Hamiltonians, which incorporate physical constraints and some parameters which are fitted to two-nucleon experimental data. Thus, the three- and four-nucleon systems constitute a special testing ground for new ideas and concepts in nuclear physics, simply because we can solve for their wave functions and because their properties have not been incorporated into our Hamiltonian models.

Of particular importance to us here is the electromagnetic interaction. Like the few-nucleon problem, electromagnetism is a relatively "clean" field, with constraints produced by fundamental principles, and with a small coupling constant which makes complicated physical processes contribute only weakly. Thus, electromagnetic interaction results are "interpretable", particularly if wave functions are accurately known. This does not imply that our work is "cut and dried", with little room for innovation. Quite to the contrary, because so much is known, electromagnetic interactions in few-body systems are the place to look for "exotic" phenomena. Because the technical aspects of the few-nucleon problem tend to obscure the many simple

results, we will concentrate in the first lecture on understanding why three-body calculations are done the way they are, in what sense they are complicated, and in what sense they are not complicated. In the second lecture we will concertrate on electromagnetic interactions involving three nucleons and other topics, including three-body forces.

Although much of the modern work in this field is formulated in momentum space, most of the older work and the work described in this lecture were formulated in configuration space (CS). Many techniques have been used to calculate CS wave functions, beginning with the august Rayleigh-Ritz variational principle[1]. Why do we and others work in configuration space? In our case the answer is simple: our physical intuition and insight are greatest there. There are, however, distinct advantages to momentum space for certain problems, such as relativistic treatments of few-nucleon systems. In what follows we will emphasize almost exclusively the bound few-nucleon systems in configuration space, and the approach of the Los Alamos-Iowa collaboration to solving the Schrödinger equation for these systems[2].

II. QUALITATIVE ASPECTS

No discussion of the three-nucleon problem is complete without a schematic discussion of the two-nucleon Hamiltonian. Many of the detailed quantitative features are irrelevant, while a few seemingly unimportant qualitative features determine most of the trinucleon properties.

The key underlying assumption is that few-nucleon dynamics is nonrelativistic. This important simplification relies on the fact that typical values of mean internal nuclear momenta, $\bar{p}$, are 100-200 MeV/c, and thus $(v/c)^2 = (\bar{p}/Mc)^2$ for a nucleon of mass Mc^2=939 MeV is one-few percent. Since $(v/c)^2$ gives the scale of relativistic corrections, this estimate would indicate that a nucleus is largely nonrelativistic. The argument hides the fact that short-range potentials can be very strong and induce local momenta which are correspondingly large; the estimate above should only be interpreted as "in the mean". Moreover, our potential models "hide" the effects of relativity in the phenomenological parts, because parameters are fit to data.

There are three salient features of the two-nucleon potential which drastically, and unfavorably, affect our ability to solve the few-nucleon Schrödinger equation. These are:

(1) Forces between like nucleons (e.g., pp or nn) are weaker than the forces between unlike nucleons (np),
(2) The two-nucleon spin-triplet potential contains a strong tensor force which couples neighboring orbital waves;
(3) The short-range force exhibits very strong repulsion, which makes the probability of nucleon-nucleon overlap at short distances very small.

Without these complications the few-nucleon Schrödinger equation is quite easy to solve. Feature (1) induces important spin and isospin correlations in the wave function. If the forces between all particles were identical, only a single (different) scalar function of the particle separations would describe each of the few-nucleon systems. With a tensor force present, the deuteron wave function has a tensor (d-wave) component, as do the triton and α-particle, which greatly complicates solving the Schrödinger equation. A strong short-range repulsion produces "holes" in the wave function. These holes must be accurately generated in any solution, which is thus rendered considerably more difficult.

In addition to these qualitative aspects of the nucleon-nucleon force, we note also that the odd-parity nucleon-nucleon partial waves (e.g., $^1P_1$, $^3P_{0,1,2}$) are relatively weak, and we will see later that they play a very small role in the triton.

A few basic principles motivate the procedures used to solve numerically various three-body problems. These are:

(1) Nuclei (including the triton) are weakly bound, and average momenta are consequently small compared to the nucleon mass;
(2) In the triton the average momentum is comparable to the inverse of the radius (R) and consequently the angular momentum barrier suppresses high partial waves of the nucleon-nucleon force;
(3) Unlike the case of heavy nuclei, the Pauli principle doesn't play a particularly large role;
(4) The details of the force are relatively unimportant in the overall binding, although they can severely complicate achieving a solution.

As we previously discussed, a nonrelativistic treatment of the triton should suffice, as indicated by (1). One estimate of the average momentum is $\bar{p} = \sqrt{M\bar{E}_b} \equiv \hbar\kappa$, where $E_b = 8.5$ MeV is the binding energy, and consequently, $\bar{p} \cong 90$ MeV/c. A typical trinucleon size is 2 fm, so that $\bar{p}R \sim 1$. Because Bessel functions of argument z and order ℓ peak for $z > \ell$, it is clear that the angular momentum barrier will greatly suppress orbital angular momenta greater than 2 in the triton.

III. GEOMETRICAL ASPECTS

The geometry of the triton illustrates the greater difficulty in solving the Schrödinger equation for the triton compared to the deuteron. The deuteron is described by a single vector $\vec{r}$ separating the nucleons, and only its magnitude is relevant for a description of the two scalar functions, u(r) and w(r), which determine the s-wave and d-wave parts of the wave function. Figure 1 shows the triton, where we have arbitrarily numbered the nucleons. Three points define a plane and thus only two vectors, $\vec{x}_1$, and $\vec{y}_1$, describe the system. Because the orientation of the plane is arbitrary, only three independent interparticle coordinates (x_1, y_1, θ_1) are required to specify the wave function. Our choice of vectors is arbitrary, however, since any set of the Jacobi coordinates formed from the nucleon coordinates $\vec{r}_i$ (i, j, k cyclic) is adequate:

$$\vec{x}_i = \vec{r}_j - \vec{r}_k \quad , \tag{1}$$

$$\vec{y}_i = \frac{1}{2}(\vec{r}_j + \vec{r}_k) - \vec{r}_i \quad . \tag{2}$$

Clearly the sums of the $\vec{x}_i$ or $\vec{y}_i$ vanish and they are linearly dependent. Traditionally, the set $(\vec{x}_1, \vec{y}_1)$ is relabelled as $(\vec{x}, \vec{y})$, where $\vec{x}$ and $\vec{y}$ are denoted the "interacting pair" and "spectator" coordinates, respectively[3].

Group theoretical methods[4] are used to classify in a well-defined way the wave function components which can occur for the positive parity, spin-½ trinucleons. Most of the important qualitative aspects of this scheme are rather obvious, however. Like the deuteron, the principal triton wave function component is s-wave in character. However, because there are several coordinates describing the problem,

this can be further broken down into three distinct categories: (1) the S-state, completely symmetric under the interchange of spatial coordinates (i.e., the $\vec{r}_i$); (2) the S′-state, which has mixed spatial symmetry (neither symmetric nor antisymmetric); (3) the S′′-state which has spatial antisymmetry. The last state has negligible size because the antisymmetry requires very large momentum components, which are lacking in the ground state, and because it is generated by the weak odd-parity nucleon-nucleon forces. The S′-state vanishes when the np, nn, and pp forces are identical, and for this reason it can be viewed as a space-isospin-(spin) correlation in the ground state. Its physical importance will be discussed later. The S-wave components are clearly spin doublet, since the trinucleons have spin ½; they are isodoublets if we ignore the Coulomb force in ^{3}He. There are also three independent spin-quartet D-wave components, analogous to the deuteron case. Unlike the deuteron case, it is possible to construct a positive parity vector ($\hat{x} \times \hat{y}$), and this leads to three quartet and one doublet P-state components, which are very small. Adding everything together, there are 10 S-, P-, and D-state components, specified by 16 scalar functions.

The Schrödinger equation for the deuteron involves 2 coupled equations in one variable (r). The Schrödinger equation for the triton is a set of 16 coupled partial differential equations in 3 independent variables. This large number of equations makes the problem roughly equivalent to a single 4-variable problem, which would require heroic efforts, even for modern supercomputers. The way to circumvent this seemingly intractable situation is to use our knowledge of the physics of the problem: the angular momentum barrier suppresses many of the problem's complexities.

Figure 2 shows two of the energy scales of the triton. The upper graph illustrates the spin- and isospin-independent MT-V nucleon-nucleon potential model[5], plotted versus nucleon-nucleon separation, x, and for comparison, the centrifugal part of the kinetic energy (for ℓ=2): $\hbar^2\ell(\ell+1)/Mx^2$. We see that the latter dwarfs the potential energy. Clearly, for higher values of ℓ this mismatch is even greater. The implications for the binding of the triton are immediate: potential

energy contributions for the higher nucleon-nucleon partial waves rapidly decrease as ℓ increases. We can easily see this by assuming a spin- and isospin-independent potential $V_{23}(x)$ between nucleons 2 and 3 and expanding this in a partial-wave series in both $\hat{x}$ and $\hat{y}$:

$$V_{23}(x) = \sum_{\alpha} |\alpha\rangle V_{23}(x) \langle\alpha| \quad , \tag{3}$$

where

$$|\alpha\rangle = [Y_{\ell}(\hat{x}) Y_{\ell}(\hat{y})]_0 \quad , \tag{4}$$

and the "channel"-label α is simply ℓ in this case. This series is much simpler than the general case, because we have assumed the same potential in <u>every</u> partial wave. Taking the expectation value of the potential between all three pairs of nucleons gives

$$\langle V \rangle = 3\langle V_{23}(x) \rangle \equiv 3 \sum_{\ell} \int_0^{\infty} dx \; x^2 C_{\ell}(x) V_{23}(x) = \sum_{\ell} \langle V_{\ell} \rangle \quad , \tag{5}$$

where the partial-wave projected correlation function is

$$C_{\ell}(x) = \int |\langle\alpha|\Psi\rangle|^2 y^2 dy \quad . \tag{6}$$

Only the completely space-symmetric S-state occurs in the wave function for this problem, and only even values of ℓ are nonvanishing because of this. The lower plot in fig. 2 shows the first four C_{ℓ}'s, which rapidly decrease in size with increasing ℓ. The dominant $C_0(x)$ is small at the origin because of the repulsion in V(x), while the remaining $C_{\ell}(x)$'s behave as $x^{2\ell}$ for small x. This means that only increasingly larger values of x contribute to the integrand in eqn. (5), which are suppressed by the finite range of the force. The values of $\langle V_{\ell} \rangle$ (for ℓ = 0, 2, ..., 10) for this simple potential model are given by [-36.6, -.163, -.019, -.002, -.0004, -.00008] MeV, dramatically illustrating the rapid convergence as ℓ increases. Clearly it should be sufficient to restrict ℓ to 4 or less. We will see later that this convergence rate also applies to more realistic potential models. We note that the sum of all the C_{ℓ}'s is the usual two-body correlation function, C(x).

By expanding the potential in a series and then truncating the series after a reasonable number of terms, we have in effect reduced the problem to solving a set of coupled equations (for the partial waves) in two variables x and y, which makes the problem tractable. A good estimate of the time scale for numerically solving the deuteron problem, starting from scratch, is one or two months. The scale for the triton bound state is perhaps two years! The problem is still very difficult, and requires a substantial commitment of personal and computer time. For future reference we note that all calculations using the Faddeev approach (to be described next) decompose the nucleon-nucleon potential into partial waves and solve that (truncated) problem "exactly".

IV. BOUNDARY CONDITIONS AND THE FADDEEV-NOYES EQUATION

We wish to solve a partial differential equation, the Schrödinger equation, for the triton bound state. It is sometimes forgotten by those who don't perform numerical calculations that such solutions require the imposition of well-defined boundary conditions. Simple bound-state problems only require the imposition of finiteness requirements for the wave function at the origin and at asymptotically large distances, where the wave function vanishes exponentially.

The scattering problem is more complex, and finiteness alone is not enough. Years ago, Foldy and Tobocman[6] showed that the three-body Lippmann-Schwinger (LS) equation (the Schrödinger equation rewritten as an integral equation) for scattering has no unique solutions, even when outgoing scattered waves are specified in the usual way. Even the two-body Lippmann-Schwinger equation has no unique solution, without further subsidiary conditions, if the the problem is posed in a particular way! The problem we pose is: what is the outgoing-wave solution for two nucleons with a total energy of 20 MeV? This is a "trick" question, because we have deliberately not specified the center-of-mass (CM) motion of the two nucleons. As stated, an arbitrary linear combination of wave functions for a deuteron with 22.2 MeV CM energy, two nucleons in a $^1S_0$ threshold state with 20 MeV CM energy, and two nucleons with an internal energy of 10 MeV and 10 MeV CM energy solves the problem. Trivially, we can avoid the problem by

working in the CM frame, which fixes the relative two-nucleon energy. Unfortunately, even in the CM frame of the three-nucleon system this does not suffice, since the recoil of a third nucleon can compensate for the CM motion of the remaining pair in any state of internal motion commensurate with conservation of energy. Because of this, complicated phenomena are possible, which makes the ad hoc imposition of boundary conditions a dubious exercise. An incoming plane wave for a proton-deuteron system (pd) can scatter directly to a pd final state, or break up into a ppn final state, or the initial proton can pick up the neutron in the deuteron and that deuteron can escape. These many physical channels are not orthogonal and specifying outgoing waves is not enough. In the jargon of few-body physics, there are "disconnected diagrams", "dangerous δ-functions", "noncompact kernels", and "nonunique solutions". All these diseases are merely symptoms of the original problem.

Of particular importance is rearrangement, such as the neutron pickup example described above. We write the Schrödinger equation in the form

$$[E-(T+V_{12}+V_{13}+V_{23})]\Psi = 0 \quad , \tag{7}$$

where T, E, and V_{ij} are the kinetic energy, total energy, and potential energy for the pair (ij), respectively. If both V_{23} and V_{13} can support a deuteron bound state, an initial plane-wave state of nucleon 1 and bound nucleons 2 and 3 [denoted (1;23)] can asymptotically become nucleon 2 plus a bound (13) pair [(2;13)]; the converse is also true and both wave functions contain both physical processes. The difficulty is that while the LS equation specifies that the (1;23) configuration has an incoming plane wave and outgoing spherical wave, it does not rule out incoming plane waves for (2;13). In order to achieve a unique solution the LS equation must be supplemented by additional homogeneous equations[7,8], which rule out unwanted incoming plane waves.

Faddeev provided the means to circumvent this dilemma[9]. Although Faddeev's procedure was developed in momentum space, Noyes[10] later cast that work into a physically equivalent configuration space form. We arbitrarily write

$$\Psi(\vec{x},\vec{y}) = \psi(\vec{x}_1,\vec{y}_1)+\psi(\vec{x}_2,\vec{y}_2)+\psi(\vec{x}_3,\vec{y}_3) \equiv \psi_1+\psi_2+\psi_3 \quad , \tag{8}$$

where the variables $(\vec{x}_i,\vec{y}_i)$ are the Jacobi coordinates defined earlier, and the function ψ in eqn. (8) is the same for all three terms. The original Schrödinger equation becomes three separate equations

$$(E-T-V_{23})\psi_1 = V_{23}(\psi_2+\psi_3) \quad , \tag{9}$$

$$(E-T-V_{13})\psi_2 = V_{13}(\psi_1+\psi_3) \quad , \tag{10}$$

$$(E-T-V_{12})\psi_3 = V_{12}(\psi_1+\psi_2) \quad . \tag{11}$$

Clearly, eqns. (10) and (11) are simply permutations of (9), and we need solve only (9). Since that equation involves only V_{23}(and not V_{13}) the problem of the rearrangement reaction has disappeared for ψ_1. It is contained in ψ_2. By this clever mechanism, Faddeev showed that we only need to specify explicitly the much simpler boundary conditions for ψ_1, rather than for Ψ. Note that the sum of eqns. (9), (10), and (11) reproduces eqn. (7).

This is seen most clearly in fig. 3, where the regions of interest for the variables x and y are illustrated. The configuration (1;23) corresponds to an asymptotic state with $y\to\infty$, and $x<x_d$, the physical extent of the bound pair (23), and is denoted the "deuteron strip". Rearrangement corresponds to small $x_2 = |\vec{r}_1-\vec{r}_3|$ (i.e., a bound state in (13)) and this occurs when $\theta = 0$, and $y = x/2$ or $\theta' = 30°$ in terms of the polar coordinates

$$x = \rho\cos\theta' \quad , \tag{12a}$$

$$y = \frac{\sqrt{3}}{2}\rho\sin\theta' \quad . \tag{12b}$$

In complete analogy with the two-body problem, we can impose boundary conditions most easily for the reduced wavefunction

$$\phi_1 = xy\psi_1 \quad , \tag{13}$$

by enforcing $\phi_1=0$ along $x=0$ and $y=0$, and outgoing wave boundary conditions[11] along $\rho=\rho_{max}$.

These physical considerations can be seen graphically in fig. 4 and fig. 5 for $\theta=0$, which depict wave functions for the scattering of zero energy neutrons and deuterons in the quartet spin state. The smooth function ψ_1 in fig. 4 has structure only along the deuteron strip, while fig. 5 depicts v_3, a component of the total wave function Ψ, which has structure along the deuteron strip and a ridge with "wings" along $\theta'=30°$, which is the outgoing wave in the rearrangement channel. It is clearly a simpler procedure to solve for ψ_1 than v_3, which has <u>much</u> more structure.

The bound-state problem[3] has much simpler boundary conditions: we need only make the wave function vanish for some large $\rho=\rho_{max}$. Nevertheless, the Faddeev motivations for the scattering problem work equally well for the bound state, and we anticipate that the Faddeev wavefunction ψ_1 will be smoother and easier to model numerically than Ψ.

Having made the decision to partial-wave project the nucleon-nucleon force, it is necessary to determine the consequence of this for the Faddeev-Noyes equation. For simplicity we assume a force which is independent of spin and isospin and acts only in the s-wave. In terms of our previous discussion, such a force looks like $|0\rangle V(x)\langle 0|$, where the projector $|0\rangle$ refers to s-waves. This produces, with $E=\hbar^2K^2/M$,

$$\frac{\partial^2}{\partial x^2} + \frac{3\partial^2}{4\partial y^2} - U(x) + K^2 \quad \phi(x,y) = U(x)\int_1^1 d\mu \quad \frac{xy}{x_2y_2} \quad \phi(x_2,y_2), \tag{14}$$

where $U(x) = MV(x)/\hbar^2$, $\mu=\cos\theta$, and $\phi(x,y) = \frac{1}{2}\int_1^1 d\mu\phi_1(x,y,\mu)$. Note that ϕ does not depend on μ; it is completely independent of θ. Moreover, for the s-wave force chosen, all higher partial waves of ϕ_1 must vanish, because V vanishes for those waves, and therefore $\Psi(x,y,\mu) = \phi(x,y) + \phi(x_2,y_2) + \phi(x_3,y_3)$. This is an extremely important result, since all of the angular (μ) dependence in Ψ comes from the permuted terms, $\phi(x_2,y_2)$ and $\phi(x_3,y_3)$, and the computation of a 3-variable function has been reduced to one of only two variables. When many

partial waves are computed, one has coupled equations in the two variables x and y. Nevertheless, the angular momentum barrier makes the required number tractable, and the calculation possible.

V. NUMERICAL MODELLING

We still must make a choice of numerical methods in order to solve the equations. A technique which has proven exceptionally powerful in modern engineering applications is the finite element method, and its variant, the method of splines[12]. Figure 6 depicts at the top a function which we wish to approximate for computational purposes, between the points x_0 and x_4, and for demonstration purposes we choose to do so by dividing the distance into 4 equally spaced regions or intervals. The finite element method consists of approximating the function in each interval by a (different) polynomial of order N and forcing the function and its first m derivatives to be continuous at the "breakpoints" between intervals. For definiteness we will choose cubic splines (N=3) involving 4 parameters, and force the function and its first derivative to be continuous. There are a total of 16 parameters, and 2 imposed conditions at each of 3 breakpoints, leaving 10 free parameters. The function is chosen to vanish at the end points, leaving 8 parameters which are chosen so that at two "collocation" points (indicated by x's) in each of the 4 intervals the function agrees exactly with the function we are modelling. If we are solving an equation for this function, we force the equation to be exactly satisfied at those points.

An alternative scheme is to use splines, which eliminates much of the labor. The finite elements in a given interval are grouped with those in a neighboring interval, which are then overlapped as shown in the middle of the figure. That is, at any point, x, the function is approximated as the sum of two overlapping functions, each defined in a double interval. These spline functions and their first m derivatives are required to vanish at the right and left ends of the double interval and to be continuous at the middle boundary. For our case (N=3 and m=1) the 8 finite element parameters for any double interval are reduced to two by these six conditions. We have graphed these (Hermite) splines as even and odd functions in the double interval, and

the remaining two parameters are simply the overall strengths of each of these functions. The beauty of this scheme is that the use of overlapping splines now guarantees that the function and its first derivative are everywhere continuous without any extra work! The boundary conditions are trivially satisfied by making the even function in the end interval vanish, and the remaining 8 parameters in the 5 overlapping spline functions are determined at the collocation points, as before. The strength of this method is that the overall number of unknowns has been reduced to the minimum before we even set up matrix equations.

The orthogonal collocation method allows one to choose the collocation points so that the power of Gauss quadratures and splines can be combined[13]. If we were to perform an integral over the function in the figure, a natural way to do this would be to integrate between breakpoints and use a Gauss quadrature formula in each interval. Using those quadrature points as collocation points constitutes the method of orthogonal collocation, which substantially improves rates of convergence when solving equations using splines.

Because splines are local functions, separately defined in each double interval, the collocation conditions couple splines from neighboring intervals only. The complete set of such conditions for all parameters (8 in our example) constitutes a matrix equation, and this matrix has a very special form because of the locality; it is a "band" matrix, with most of the elements zero, as shown at the bottom of fig. 6. Such matrices are much easier to invert than dense matrices, and should be preserved, if possible. In order to deal with the angular integral in eqn. 14, we transform from (x,y) coordinates to the polar coordinates (ρ,θ'). The integral destroys the double band structure in x and y; polar coordinates preserve this structure in the variable ρ.

There are a number of important advantages which accrue from using splines to model a function: (1) The spline approximant and a specified number of derivatives are automatically continuous; (2) The splines automatically provide an interpolating function at any point; (3) They lead to a band matrix; (4) They are "optimally" smooth; (5) It is easy to change from the equally spaced intervals of our example to

any desired distribution; (6) The splines are easy to program on a computer; (7) Boundary conditions are easy to impose; (8) The approximants exactly satisfy the constraint equations at the collocation points; (9) Piecewise local functions such as splines do not propagate approximation errors, as global functions do; (10) The relative accuracy of the wave function and eigenvalue should be comparable. We also note that the use of overlapping double intervals corresponds closely to one derivation of the powerful Gregory's integration rule from Simpson's integration rule.

There is little difference in principle between solving eqn. (14) for a single nucleon-nucleon (NN) partial wave and using many partial waves. The size of the matrices becomes much larger, and the matrix bookkeeping becomes very tedious and intricate. In general for each nucleon-nucleon partial wave, there are two spectator partial waves associated with the two spin states of the latter, except for total angular momentum, J, equal to zero, which generates only one. The four NN partial waves ($^{S}L_{J}$) for each J ($^{1}J_{J}$,$^{3}J_{J}$,$^{3}J\text{-}1_{J}$,$^{3}J\text{+}1_{J}$) thus generate 8 trinucleon channels, except for J=0, which has only two, associated with $^{1}S_{0}$ and $^{3}P_{0}$. As we indicated earlier, the $^{1}S_{0}$ and $^{3}S_{1}$ waves should be dominant, and we must also include the $^{3}D_{1}$ wave, which is strongly coupled by the tensor force to the $^{3}S_{1}$ wave. This combination is the standard 5-channel calculation (all positive-parity NN waves with $J\leq 1$). The 9, 18, 26, and 34 channel cases correspond to positive parity waves with $J\leq 2$, all waves with $J\leq 2$, positive parity waves with $3\leq J\leq 4$ waves, and all waves with $J\leq 4$, respectively.

VI. RESULTS FOR TRINUCLEON BOUND STATES

A brief summary of results[14] for the Reid Soft Core[15] (RSC), Argonne[16] V_{14} (AV14), Super-Soft-Core(C)[17] [SSC(C)], and Paris[18] potential models is given in Table 1 as a function of channel number. Several conclusions are obvious: (1) The 5-channel approximation gives most of the binding (within .2-.3 MeV); (2) The negative-parity NN waves don't have a large effect; (3) The binding is roughly 1 MeV below experiment; (4) The point-nucleon rms charge radii (i.e., the proton radii) for ^{3}He and ^{3}H are larger than experiment. Because the positive-parity waves dominate, this table doesn't demonstrate the rate

of convergence of the partial-wave series. This is shown in Table 2 for the RSC 34-channel case, where <V> is broken down into contributions for fixed J and fixed parity. All but 1% of the total potential energy (indicated by Σ in the last column) is generated by the first 5 channels, and most of the rest from the remaining positive-parity waves. The small negative-parity $N\bar{N}$ forces give 200 keV more binding, which is not obviously reflected in Table 1 (compare 18 channels to 9 channels). The reason is that the negative-parity forces couple directly to the small components of the wave function and this leads to nearly cancelling contributions from first- and second-order perturbation theory. First-order perturbation theory works well for all the other small force components.

The probabilities of the important S'- and D-state wave function components are small. The D-state probabilities for the triton are very nearly 3/2 times the corresponding D-state probabilities of the deuteron for each potential model.

Table 1. Binding energies, point charge rms radii in fm, and percentages of wave function components for various two-body force models.[17]

	-E (MeV)					$\langle r^2\rangle^{\frac{1}{2}}_{He}$	$\langle r^2\rangle^{\frac{1}{2}}_{H}$	P_S	P_D
Model	5	9	18	26	34	34	34	34	34
RSC	7.02	7.21	7.23	7.34	7.35	1.85	1.67	1.40	9.50
AV14	7.44	7.5[illegible]	7.57	7.67	7.67	1.83	1.67	1.12	8.96
SSC(C)[19]	7.46	7.52	7.49	7.54	7.53	1.85	1.68	1.24	7.98
Paris[19]	7.30		7.38						
Expt.		8.48				1.69(3)	1.54(4)	--	--

Table 2. Potential energies (in MeV) for the RSC 34-channel case broken down according to J (total nucleon-nucleon angular momentum) and parity, and the kinetic energy for comparison.

J	0	1	2	3	4	Σ
$\langle V_J\rangle$	-13.729	-43.647	-0.435	-0.115	-0.020	-57.946
$\langle V_J^+\rangle$	-13.553	-43.874	-0.188	-0.117	-0.014	-57.746
$\langle V_J^-\rangle$	-0.176	0.227	-0.247	0.002	-0.006	-0.200
<T>						50.600
<H>						-7.345

Clearly there is underbinding, and the radii aren't correct either. The latter and other important observables depend on the binding energy, and since that is wrong the observables can't be correct. In order to investigate this problem which has plagued us for a decade, we anticipate some of the results of the next section, and introduce a three-body force to increase binding. We don't need to know what it is at this stage. Our study of these observables will allow us to gain a qualitative understanding of them at the same time.

Although a wide variety of bound-state calculations have been performed during the previous two decades for a variety of potential models, many produced only binding energies and no wave functions, and others required approximations whose reliability was difficult to assess. The recent studies[20] of the Los Alamos-Iowa group have produced a large number of numerically accurate triton wavefunctions for four different two-body potential models in combination with several different three-body force models, each calculated for various numbers of channels. Although there is no guarantee that these model combinations accurately describe nature, the solutions at least incorporate the correct qunacum mechanical constraints. Moreover, the binding energies for the set of models extend from below to above the physical binding energy of the triton. This provides us for the first time with the opportunity to investigate how a variety of important ground-state observables depend on the binding energy, and whether there is any "true" model dependence as well.

What are the important ground-state properties, besides the binding energy? A list of the most commonly calculated ones would include the (point) charge radii, $\langle r^2 \rangle^{\frac{1}{2}}_{He}$ and $\langle r^2 \rangle^{\frac{1}{2}}_{H}$, the probabilities of the various wave function components (which are not measurable[21]), the Coulomb energy of ^3He, E_c, the magnetic moments of ^3He and ^3H, their asymptotic norms (sizes of asymptotic wave function components), and the β-decay matrix element of ^3H. The magnetic moments depend on meson-exchange currents and on the S'- and D-state probabilities, $P_{S'}$ and P_D, as does the β-decay matrix element; we will discuss them later. The asymptotic norms depend on binding, but this has not been assessed in detail yet. The radii and Coulomb energy depend sensitively on the

binding energy, and calculations of these observables which use models that underbind will produce inadequate predictions. We assess the status of these important physical quantities below, together with simple qualitative arguments that account for our conclusions.

For pedagogical purposes, the difference of the ^{3}He and ^{3}H charge radii can be understood in terms of the oversimplified pictures in fig. 7. The sketch at the top depicts a schematic ^{3}He when the nucleon-nucleon forces between all pairs are identical. This is represented by an equilateral triangle configuration, with shading depicting the protons. The charge or proton radius, R_p, measures the integrated probability of finding a proton at a distance r from the center-of-mass. In this simple example, the proton, neutron, and mass radii are all the same. When the forces between pairs are different, the appropriate pictures for ^{3}He and ^{3}H are those of fig. (7b) and fig. (7c). The np forces are stronger than the nn or pp ones (only the np system has a two-body bound state) and this allows the protons in ^{3}He and the neutrons in ^{3}H to lie further from the the center-of-mass than their counterparts ($\theta>60°$). The resulting isosceles configuration is reflected in the appearance of an S'-state, which directly measures the isosceles-equilateral difference, and in the fact that R_p for ^{3}He increases, while that of ^{3}H decreases, and hence $\langle r^2\rangle^{\frac{1}{2}}_{He} > \langle r^2\rangle^{\frac{1}{2}}_{H}$, irrespective of any pp Coulomb force in ^{3}He.

These arguments can be made quantitative by decomposing the mean-square-radius in impulse approximation into isospin components[22]: the isoscalar part $\langle r^2\rangle_s$ mirrors fig. (7a) and is determined by sums of squares of wave function components. The isovector component contains one part proportional to the isoscalar component and another part largely determined by the overlap of the S- and S'-states, which we denote $\langle r^2\rangle_v$ (v does <u>not</u> mean isovector), and determines the difference between ^{3}He and ^{3}H. One finds for ^{3}He (Z=2) and ^{3}H(Z=1), with upper and lower signs, respectively,

$$Z\langle r^2\rangle = Z\langle r^2\rangle_s \pm \langle r^2\rangle_v \quad . \tag{15}$$

These quantities have very different behaviors. Radii in general are sensitive to the asymptotic parts of the wavefunction. If one assumes

that the entire wavefunction is represented by the asymptotic form[3], $N \exp(-\kappa\rho)/\rho^{5/2}$, one finds that

$$\langle r^2\rangle_s^{\frac{1}{2}} = \frac{1}{2\kappa} \sim E_B^{-\frac{1}{2}} \quad . \tag{16}$$

Figure 8 shows the results of calculating $\langle r^2\rangle_s^{\frac{1}{2}}$, and $\langle r^2\rangle_v^{\frac{1}{2}}$, together with the experimental data corrected for the nucleons' finite size[2]. The fit to the isoscalar points is accurately represented by $.8E_B^{-.5}$, indicating that our simple argument was essentially correct. The difference radius is fit by $.14E_B^{-.9}$, and this different behavior reflects different physics. Clearly , the amount of S'-state plays a significant role. The percentage of S'-state is plotted versus binding energy in fig. 9, and the fit varies as $E_B^{-2.1}$ This decrease is expected, because as binding increases only the average force is important, and the np-nn difference is less important. In a simple harmonic oscillator description, the S'-state is given in terms of excited state configurations, which decrease $\sim E_B^{-2}$ as the oscillator spacing increases with binding. Finally, the ^{3}He and ^{3}H results are shown in fig. 10. If the small discrepancies between theory and experiment are real, they probably reflect a small breakdown of the impulse approximation.

The Coulomb force $V_c(x)$ between protons in ^{3}He is quite weak and can be accurately treated in perturbation theory. The second-order Coulomb effect[23] is estimated to be ~-4 keV, compared to a ^{3}He-^{3}H binding energy difference of 764 keV. Since $V_c \sim 1/R$, schematically, and since $R \sim E_B^{-\frac{1}{2}}$, we expect E_c to scale roughly as $E_B^{\frac{1}{2}}$. A better description is available, however, if we utilize fig. (7a). In this schematic ^{3}He the distance x between protons is given by $\sqrt{3}r$, and thus $E_c = \langle V_c(x)\rangle = \alpha\langle 1/r\rangle/\sqrt{3}$, where α is the fine structure constant. Consequently[24],

$$E_c \cong \frac{\alpha}{\sqrt{3}}\int\frac{d^3r}{r}[\rho_s(r) + \rho_v(r)]g(r) = E_c^H \quad , \tag{17}$$

where we have added the effect of nucleon finite size[22], g(r), and written the matrix element in terms of the scalar and difference

charge densities. The accuracy of this hyperspherical approximation is demonstrated in fig. 11. Although a priori a very implausible approximation, E_c^H overestimates E_c by only 1 percent. This is an important result, because the charge densities are experimentally measurable. Using these data[22] one finds $E_c = 638 \pm 10$ keV. This is significantly less than the binding energy difference and reflects the existence of nonnegligible charge-symmetry-breaking forces other than the Coulomb interaction.

VII. CONCLUSIONS

Rapid and significant advances have been made in the few-nucleon problem recently. Many aspects of the bound states, including the Coulomb energy and charge radii, are now fairly well understood. Although we have concentrated on the trinucleon bound states, the continuum is also important. Photonuclear reactions necessarily break up the triton and ^{3}He, and this is an important area of study. The continuum problem above breakup threshold is much more complicated than the bound-state problem, because the boundary conditions are difficult to implement in a tractable way. Nevertheless, the future of three-body physics lies in this regime.

LECTURE 2. TRINUCLEON INTERACTIONS

I. NONTRADITIONAL NUCLEAR PHYSICS

For much of its 50 year existence nuclear physics has made tacit assumptions in its approach to problem solving. These assumptions, which comprise what I call traditional nuclear physics, are:

1) Nuclei are basically nonrelativistic and weakly bound, with average momenta being typically 100-200 MeV/c;
2) The binding of nuclei is produced primarily by two-body forces, which act only between pairs of nucleons at a time;
3) Only nucleon degrees of freedom are important, and nucleon substructure and meson or quark degrees of freedom can be ignored.

Although there were some early challenges to this approach to our field, it was only in the late 1960's that a serious, concerted effort was made to find exceptions to these "rules". The problem was that traditional nuclear physics was reasonably successful. Moreover, the curse of nuclear physics and related fields is our inability to accurately solve the many-body problem beyond the mean-field approximation, which meant that disagreements between theory and experiment were difficult to interpret. Were they due to poor wavefunctions, or to a poorly understood reaction mechanism?

The importance of the few-nucleon problem can be understood in this context. At the same time that modern intermediate energy (i.e., nontraditional) nuclear physics was being developed, great strides were being made in the few-nucleon problem. The early calculations by Tjon and collaborators[5] and by Kalos[25] used modern computational methods to solve for binding energies and wave functions; the latter were then available for computing electromagnetic matrix elements. This is still the strength of the field. We can solve the Schrödinger equation "exactly" for wave functions, and use the wave functions in calculations of electromagnetic processes, which are the most "interpretable" of all the types of reactions available to nuclear physicists. This is also our challenge for the next decade.

We have already estimated the size of relativistic corrections to be on the order of one to a few percent. The best evidence for

relativistic corrections in low-energy nuclear reactions occurs for deuteron forward photodisintegration[26], where the proton is detected at 0°. This configuration greatly suppresses the dominant non-relativistic electric dipole (E1) reaction, so that a nominally one percent relativistic correction becomes a 20 percent effect! This points out one of the difficulties in challenging traditional nuclear physics: novel reactions or special regimes of known reactions must be sought in order to suppress the "ordinary" physics. The importance of relativistic effects will arise again in the context of three-nucleon forces.

One of the biggest success stories in all of nuclear physics during the decade of the 1970's was the convincing demonstration of meson degrees of freedom in electromagnetic reactions, and in particular, of the importance of the pion in exchange currents. Much of that story revolved around the threshold deuteron photo- and electro-disintegration and np radiative capture, all of which are magnetic dipole (M1) processes. Riska and Brown[27] calculated the dominant pion-exchange processes and showed that the long-standing 10 percent discrepancy in np radiative capture could be largely understood from those processes alone. Moreover, many of the uncertainties in the pion's strong interaction had been eliminated as the consequences of chiral symmetry[28], which singles out the pion as a special particle, had unfolded during the decade of the 1960's. The possible importance of such meson-exchange currents had been known since the 1930's, when Siegert[29] demonstrated that the long-wavelength E1 current operator could be written in a form involving only the electric dipole operator (calculated from the charge density), which was shown to be accurately known in the nonrelativistic approximation. This combination is known as Siegert's theorem and is the backbone of photonuclear physics, because it allows a simple interpretation of reactions. Magnetic processes are very model dependent and sensitive to details of the current, while Siegert's current is not.

In what follows we will investigate in some detail in the context of the three-nucleon problem two of the nontraditional elements we listed earlier: three-nucleon forces and meson-exchange currents. We will see that both are linked to relativistic corrections and to each

other. Regrettably, we must leave the interesting two-body problem to others.

II. THREE-BODY FORCES

A. Introduction

Before considering the evidence for three-body forces in nuclei, we first discuss whether such forces exist in other systems, and how they are defined. Most of the weaker fundamental forces, gravitational and electromagnetic, are basically two-body in nature. The considerations of Newton and Coulomb were based on that assumption. Is this assumption valid? We give two answers, which we will discuss in detail: (1) It is an excellent approximation; (2) It depends on your point of view.

We begin with a classical example, the earth-moon system with a small satellite orbiting the earth. We also assume, as Newton did, that each tiny particle of mass (aton) interacts with every other by two-body forces; that is, the interaction between two such particles is not affected by the presence of a third. This by itself is not enough to be able to solve for the coupled motion of our classical system, since there are enormous numbers of atoms in the problem we posed. It was Newton's genius that allowed him to see that the interaction of large bodies could be constructed from that of the individual tiny pieces, after he invented the necessary mathematics! We therefore reduce the problem to one of three macroscopic bodies interacting with each other. Does the position of the moon affect the force between the satellite and the earth? If one neglects the tides, the answer is no, and the problem is simply one of 3 separate two-body forces between composite objects. However, the tides caused by the moon affect the satellite motion in an observable way[30], and the position of the moon is clearly relevant, which means that the earth-moon satellite system exhibits a three-body force mediated by a deformation of the earth, namely the tides. The effect is very small, however.

A second example of three-body forces is the atomic Axilrod-Teller force[31]. Many-body calculations with groups of atoms are traditionally performed by assuming an effective interaction between atoms, rather than breaking the problem down into purely Coulombic two-body

interactions between all the nuclei and electrons in all the atoms, which is much too complicated. Typical of two-body atom-atom interactions are the long-range van der Waals force, and the Lennard-Jones force. Having arranged the problem in this way, there will be forces between three atoms, between four atoms, ... , which arise from mutual distortion.[32] The long-range three-atom force is the Axilrod-Teller force, whose most salient feature is the strong dependence that it has on the relative angular orientation of the atoms. This is very typical of three-body forces, whatever their origin, and was a feature of our classical example. This property will be important to us later.

We see that many three-body forces are largely a matter of definition, rather than fundamental. In order to make calculations tractable, we deal with the interactions of composite systems, rather than their constituents. Although the constituents may interact via two-body forces, the composite objects can interact via effective many-body forces. For our purposes we define three-nucleon forces as those forces which depend in an irreducible way on the simultaneous coordinates of three nucleons, when only nucleon degrees of freedom are taken into account. One new element appears in our definition, the word "irreducible". In our classical example we separated the total force into two-body forces between pairs of objects (e.g., satellite-earth) and whatever was left over. It is important not to confuse the sequential interactions of two-body forces as a three-body force; that is the meaning of "irreducible". It is a simple concept but a complicated technical matter to put it into practice[33], and the latter requires much more time than we have here.

This brief introduction to a fascinating subject brings us to the topic of interest: three-nucleon forces. The types of processes which can contribute are illustrated in fig. 12. We are primarily interested in pion-range forces, since the pion has the longest range ($\sim\hbar/\mu c$, where μ is the pion mass). We hope, on the basis of arguments to be presented later in connection with exchange currents, that the longest-range forces will dominate. Figure (12a) shows the generic two-pion-exchange three-nucleon (2π-3N) force. A π^+ is emitted by the proton on the left, propagates and scatters from the middle nucleon (the "blob"

represents the scattering mechanism), then turns into a π^0 which is absorbed by the rightmost proton. The many possible combinations of pion charges means that this force has a complex isospin structure. Because we are dealing with pions, it also has a complicated spin structure. Moreover, the pion is not real, but virtual or "off-shell". Figures 12b-f are possible components of fig. 12a. The second process is "reducible"; that is, it looks like two sequential exchanges of a pion, and hence is not fundamental. It must be discarded. Note that this reducible graph can be cut in two without breaking anything but nucleon lines. The next process is similar to the classical example; the second nucleon is "deformed" into an isobar by the pion exchange and leads to the conceptually important isobar-meditated three-body force. Figure 12d has an intermediate nucleon-antinucleon pair, and leads to a force which is conceptually the same (but not structurally) as the atomic Primakoff-Holstein three-electron force[34]. In figs. 12e and 12f the pion scatters from virtual mesons. The three-isobar force shown next is a 3π-3N force, which is conceptually similar to the Axilrod-Teller atomic force, because it is produced by the mutual distortion of three nucleons. The remaining processes can also contribute to 2π-3N and 3π-3N forces.[2]

B. Evidence

The results presented earlier strongly indicate that there is a defect in binding from conventional two-body forces. Moreover, the too large (calculated) radii are likely a symptom of this same problem, as we saw. There are several plausible explanations: (1) Relativistic corrections have not been calculated; (2) Three-body forces, which depend on the simultaneous coordinates of all 3 nucleons in the triton, have not been included; (3) Our model Hamiltonians are simply inadequate, and the effects of nucleon structure or meson degrees of freedom should be taken into account. In fact, these categories are not distinct. Relativistic corrections can be broken down into one-body (kinetic-energy) terms, two-body (potential-energy) terms, and three-body (and higher) potential-energy terms. The size estimate we previously made of relativistic corrections (1-few percent), taken for the kinetic or potential energies (±50 MeV), predicts a scale of 0.5-1 MeV. Those calculations that have been performed on the one- and

two-body parts are consistent with this estimate, but find a tendency for cancellation between the attractive kinetic-energy correction and a repulsive potential-energy correction, leaving a small residue. It is also known that a substantial part of the two-pion-exchange three-body force is a relativistic correction[33] of order V_π^2/Mc^2, where V_π is the usual one-pion-exchange potential (OPEP). Moreover, the isobar part of the former force shown in fig. 12c is due to nucleon substructure: a pion emitted by nucleon 1 (virtually) polarizes nucleon 2 into an isobar, which decays back to a nucleon plus a pion, which is absorbed by nucleon 3. Most of the currently popular three-nucleon forces[35-39] have been derived by considering meson degrees of freedom. These forces clearly exist in nature, but are they large enough to solve our binding problem?

Another long-standing problem has been a good theoretical understanding of the ^{3}He charge form factor, or the Fourier transform of the charge density. The form factor, (fig. 22, to be shown later), has a typical diffraction shape, as a function of q, the momentum transfer, falling rapidly through zero, becoming negative in the secondary maximum, and then positive again. The difficulty has been that theoretical calculations have predicted too small a (negative) strength in the secondary maximum. The point-nucleon charge density $\rho_{ch}(r)$ constructed from the experimental form factor $F_{ch}(q^2)$ is consequently much lower than theoretical calculations near the origin[40], as shown in fig. 13. This follows from the Fourier transform relationship

$$\rho_{ch}(0) = \frac{1}{2\pi^2} \int_0^\infty F_{ch}(q^2) q^2 dq \quad . \tag{18}$$

Clearly a large negative contribution to F_{ch} lowers $\rho_{ch}(0)$. The argument that we have presented is somewhat controversial[2], because values of F_{ch} for very large q are needed in order to make the integral converge, and this requires considerable theoretical assumptions and extrapolation, some of which may be dubious. Nevertheless, there is a problem with the form factor, as we will see later.

In impulse approximation the charge density measures the probability of finding a proton at a distance r from the trinucleon

center-of-mass, indicated by the x in fig. 1. Taking nucleon 1 to be that proton, we have $r = \frac{2}{3}y$, and forcing r to zero makes y zero. This is the condition for all three nucleons existing in a collinear configuration. Binding, on the other hand, prefers equilateral or isosceles configurations, so that each nucleon can be attracted by the short-range force of each of the other nucleons. Both of our problems with experiment could be solved if the three-nucleon force were attractive for equilateral configurations and repulsive for collinear ones. Schematic models of the force have this structure, and produce both effects, although other models may not. We note that r=0, or y=0, does not correspond to the "hole" in the wavefunction produced by the strong short-range repulsion. The S-state component of the wavefunction for $\theta=0°$, corresponding to a 5-channel RSC potential calculation, is shown in fig. 14. The deep valley at $\theta'=30°$ reflects that repulsion, while $\rho_{ch}(0)$ is given by an integral over x, along y=0. This Schrödinger wavefunction is generated by the much smoother Faddeev wave function component ψ_1^S shown in fig. 15.

In addition to bound states, the trinucleons have a rich continuum structure. At very low (essentially zero) energy the scattering of a nucleon from the deuteron can be characterized by a single observable, the scattering length, a, which can be decomposed into spin-doublet (a_2) and spin-quartet (a_4) components. The latter is quite uninteresting, because it seems to depend only on the deuteron's binding energy due to the effect of the Pauli principle in the quartet state; consequently, all "realistic" force models produce nearly the same result. Calculated doublet scattering lengths, on the other hand, have been too large. Typical values are shown in fig. 16, where a_2 has been calculated[41] for a variety of realistic and unrealistic two- and three-body force models. These results for pd and nd scattering separately fall on "Phillips lines"[42] when plotted versus the corresponding triton or ^{3}He binding energy. The fit to the nd results passes through the experimental datum; the pd result does not, which is a mystery at this time. The fact that all of the nd doublet results track the same Phillips line indicates that whatever physical mechanism corrects the binding defect will also produce a correct value for a_2, at least for the nd case.

Finally, analyses of the nn-scattering length, a_{nn}, from two separate experiments, n+d→(n+n)+p and π^-+d→(n+n)+γ, have produced three different values of a_{nn}. It has been argued[43] that three-nucleon forces, conspicuously missing in the latter reaction and not included in the analyses of the former reaction, might produce agreement among the values of a_{nn} from the different reactions. Only schematic calculations have been performed to date[44].

The evidence we have presented is tantalizing, but it is at best circumstantial. At present the best evidence exists in the properties of the bound state. Can current models of the three-nucleon force produce a substantial increase in binding? At least four such models have been used recently: (1) the Tucson-Melbourne (TM) two-pion-exchange force[35]; (2) the Brazilian (BR) two-pion-exchange force[36]; (3) the Urbana-Argonne (UA) schematic force[37]; (4) the Hajduk-Sauer isobar model[38]. Hajduk and Sauer do not explicitly include a separate three-body force in their model, but rather include isobar components in their wavefunctions. Three-body-force contributions, implicitly included in their model, must be deduced later. The TM and BR models incorporate figs. 12c-12f into their forces.

C. Calculations

The early calculations used different force models and various approximations, which resulted in a chaotic situation, some calculations finding negligible additional binding and others finding more than one MeV. The situation has recently been clarified in part[45]. Most calculations had resorted to perturbation theory using 5-channel wave functions[46], which fails badly. Perturbation theory is inadequate for the TM model, giving results which are much too small. The 5-channel wave function approximation is also inadequate in general, as noted by Hajduk and Sauer[39], because the pion-exchange potentials tend to couple to small wave function components not adequately represented in the 5-channel approximation; 34 channels are required for complete convergence[45]. The latter calculations found approximately 1.5 MeV additional binding from both the TM and BR forces, in combination with two different two-body force models. Calculations of $\rho_{ch}(0)$ are not completed.

Although these results indicate a substantial three-body force effect, caution is required. Hajduk and Sauer find a small (-.3 MeV) three-body force effect. Their approach is very different from the TM and BR groups, and the physical reasons for the discrepancy are not known. Moreover, the "long-range" two-pion-exchange force is unfortunately quite sensitive to its short-range behavior, and it is possible to substantially lower the binding by making plausible modifications of this behavior. This field is in its infancy and much more work needs to be performed.

Finally, fig. 17 shows a possible scheme[47] for determining the size of three-body forces by exploiting its angular dependence in the continuum. The initial pd configuration can be broken up into a p+p+n final state, which is measured in an equilateral configuration (b) and in a collinear one (c). This very difficult experiment might shed light on such forces, by looking for the expected additional attraction in the former configuration and repulsion in the latter.

III. ELECTROMAGNETIC INTERACTIONS

A. Relativistic Corrections

If relativistic effects are corrections (rather than dominant), an expansion of operators[48-49] in powers of (v/c) could prove useful in explicating the physics of various processes. The nonrelativistic charge operator (ρ_0) has the form

$$\rho_0(\underline{x}) = \sum_{i=1}^{A} e_i \delta^3(\underline{x}-\underline{x}_i) \quad , \tag{19}$$

which confines the charge at a point $\underline{x}$ to those nucleons located at $\underline{x}_i$ with $e_i = 1$ (protons), rather than $e_i = 0$ (neutrons). The classical current operator has two components,

$$\vec{J}_0(\underline{x}) = \sum_{i=1}^{A} e_i \{\frac{\vec{p}_i}{2Mc}, \delta^3(\underline{x}-\underline{x}_i)\} + \vec{\nabla}\times \sum_{i=1}^{A} \frac{\mu_i \vec{\sigma}(i)}{2Mc} \delta^3(\underline{x}-\underline{x}_i) \quad , \tag{20}$$

where e_i, μ_i, $\vec{p}_i$, and $\vec{\sigma}(i)$ are the charge, magnetic moment (in nuclear magnetons), momentum, and (Pauli) spin operators for nucleon i, and M

is the common nucleon mass. The first term is the convection current, produced by charges moving with velocity $\vec{p}/M$. The second is the magnetization current, produced by the elementary "bar magnets" that are the individual nucleons. Note the explicit factor of 1/Mc in each. The currents are smaller than the charge by factors of 1/c and 1/M, and M is a large number on the scale of nuclear momenta.

In order to count powers of 1/M as equivalent to powers of 1/c, we must use the fact that nuclei are weakly bound, and the potential and kinetic energies ($p^2/2M$) are nearly equal and opposite. Consequently, we expect momentum-(kinetic) and potential-dependent operators of the same order in (1/c) to be comparable. For both these reasons we reckon potential energy as order (1/M), and thus a series in 1/M is the same as a series in 1/c. These are our "rules of scale".

Corrections to the charge operator ρ_0 (order $(1/c)^0$) are of order $1/c^2$, or $1/M^2$, as originally argued by Siegert[29]. They include[26] the spin-orbit interaction charge density, the Darwin-Foldy term, and various meson-exchange contributions. The spin-orbit and Darwin-Foldy terms play an important role in the charge density differences of isotopes[48], and the former produces a relativistic correction to the dipole operator, which is the dominant such correction to deuteron forward photodisintegration. Corrections to the current operator are of order $1/c^3$ (or $1/M^3$), and higher. They include meson-exchange contributions. The scheme we have listed here, with the components of the charge operator being of order $(1/c)^0+(1/c)^2+ (1/c)^4+ \ldots$, and the current being of order $(1/c)+(1/c)^3+ \ldots$, is not the only one possible, in general. The other possibility is for the leading-order current to be of order $(1/c)^0$ and the charge to be of leading order (1/c). The former type of current, whose archetype is the electromagnetic or vector current, is denoted[49] class I, while the latter is termed class II. Does any simple example of the latter class exist? The answer is yes and is exemplified by the axial vector current, which is important in β-decay. The Gamow-Teller β-decay operator is the axial current, $\vec{J}_A$, and is of nonrelativistic order, $(1/c)^0$.

B. Current Conservation and Exchange Currents

The nonrelativistic currents we wrote in eqn. (20) are also the standard currents of atomic physics. They do not depend on the binding potential. Is the same true for nuclear physics? The answer is no, and points out an important qualitative difference between nuclear and atomic physics: binding in atomic physics is accomplished via exchange of <u>neutral</u> virtual quanta (photons), while in nuclear physics at least half of the binding arises from the exchange of charged quanta (e.g., mesons). The difference is qualitative, because the motion of any charged particle generates a current in both classical and quantum physics. In a weakly bound system of heavy particles, the binding quanta (mesons) move very rapidly compared to the nucleons, and hence the charge is largely confined to the heavy particles. The charge operator in eqn. (19) simply reflects this statement. Meson-exchange corrections to ρ_0 arise from nucleon recoil and the finite time of propagation of the mesons between nucleons, and are at least second order in $1/c^2$. On the other hand, the weak binding argument we produced earlier would indicate that the nonrelativistic nuclear current gets large (50% to 100%) contributions from potential-dependent currents. This estimate turns out to be too high because of an accident of nature. The big exchange-current effects in the two-body problem we discussed earlier were found in isospin-changing (isovector) magnetic dipole transitions, and primarily involve the magnetization current. The isovector part of that current is proportional to the isovector nucleon magnetic moment, $\mu_v^o = \mu_p - \mu_n = 4.71$ n.m., whose large size suppresses the fractional exchange-current contribution. Were μ_v^o of "normal" size like the isoscalar moment, $\mu_s^o = \mu_p + \mu_n = 0.88$ n.m. , exchange-current effects in nuclei would be typically 50%!

The single most important theoretical aspect of electromagnetism is gauge invariance, which follows from the masslessness of the photon. It must be possible to make a photon's wave function orthogonal to the Poynting vector (i.e., transverse) in any frame of reference, because the photon's helicity is an observable. A Lorentz transformation can alter the photon's wavefunction, however, and gauge invariance is the condition which restores transversality. For processes which involve

only a single photon, real or virtual, gauge invariance is exactly equivalent to conservation of the electromagnetic current, whose components are ρ and $\vec{J}$:

$$\vec{\nabla}\cdot\vec{J}(\underset{\sim}{x}) = -i[H,\rho(\underset{\sim}{x})] \quad , \tag{21}$$

where H is the strong interaction Hamiltonian.

If we write H = T+V, where T and V are the kinetic and potential energies, and use isospin notation for $e_i = (1+\tau_z(i))/2$ in eqn. (19), we see that those parts of the potential between nucleons i and j which are isospin dependent $[(\vec{\tau}(i)\cdot\vec{\tau}(j))V_{ij}]$ will not commute with ρ, and hence there must be exchange or potential-dependent currents in $\vec{J}$ to make current conservation possible. The strong isospin dependence of the force guarantees large exchange currents, as we previously argued. We note that the magnetization current is divergenceless (solenoidal), and the convection current satisfies eqn. (21) in conjunction with the kinetic energy, T.

The existence of these currents does not mean that we can calculate them. Indeed, we are faced with the same problem that has confronted nuclear physics from its beginnings: without a tractable model of the strong interactions, we are able to calculate only in perturbation theory, which does not obviously converge. Fortunately, an accident of nature rescues us from this dilemma. The nucleon-nucleon interaction is strongly repulsive for small separations, and this makes the probability of finding nucleons in such configurations very unlikely. It also means that the matrix elements of any short-range current operators are greatly suppressed, and the longest-range operators should dominate. This is illustrated in fig. 18, which shows the two-body trinucleon correlation function C(x), formed by integrating $|\Psi|^2$ over y and $\hat{x}\cdot\hat{y}$. Exchange currents would contribute to the ground state proportional to $\int C(x)\vec{J}(x)x^2dx$. The maximum value of C(x) falls between one- and two-pion-range as indicated by the arrows, and ρ-meson range corresponds to a very small value of C(x). The additional factor of x^2 in the volume element further accentuates the long-range operators. We expect on the basis of these arguments that the longest-range currents, the one-pion-exchange (OPE) currents, should dominate, and explicit calculations bear this out.

The pion's mass is much smaller than that of any other meson, which appeared to be accidental until the discovery of (approximate) chiral symmetry. Not only does that symmetry account for the small mass, it places constraints on the pion's interactions[50] with other hadrons, which allows many calculations to be performed that would otherwise be dubious. Because OPE currents play the dominant role in exchange currents, and because of their past and continuing importance in our field, we derive them from "first principles" in the following section.

C. One-Pion-Exchange Currents

Figure 19 shows the four dominant processes involving the exchange of a single pion. Figure 19a depicts the OPE potential arising from π^+ exchange. In addition there are contributions from π^- and π° exchange. In few-nucleon systems the OPE potential is extremely important, and dominates the binding; it is attractive and has a very strong tensor force. Figures 19b-19d show how a pion influences the electromagnetic interaction of a nucleus: the cross and wiggly line denote an external electromagnetic interaction, which produces a pion (photopion production) on one nucleon that is later absorbed by a second nucleon. Processes (b), (c), and (d) are the "seagull", "true-exchange", and "isobar" portions of the pion-exchange current.

Because of their importance, we will derive the operators corresponding to fig. 19. We are only interested in the nonrelativistic portions of these processes and consequently work in the static limit ($M\to\infty$). The basic building block we need is the pion-nucleon vertex, $j_\pi^\alpha(\underline{x})$, two of which comprise OPEP. Because the pion has three charge states (π^+,π°,π^-), the vertex must be an isovector, indicated by the (isovector) index α. This vertex determines the probability of a virtual pion, whose wave function is $\phi_\pi^\alpha(\underline{x})$, being emitted from nucleon 1 at the point $\underline{x}$:

$$H_{\pi NN} = \int \psi_f^\dagger(\underline{x})\; j_\pi^\alpha(\underline{x})\; \psi_i(\underline{x})\; \phi_\pi^\alpha(\underline{x})\; d^3x \quad , \tag{22}$$

where

$$j_\pi^\alpha(\underset{\sim}{x}) = \frac{-f}{\mu}\,\vec{\sigma}(1)\cdot\vec{\nabla}_1\delta^3(\underset{\sim}{x}-\underset{\sim}{x}_1)\;\tau^\alpha(1) \quad . \tag{23}$$

The integrated probability of a pion of mass μ and charge state α being emitted by a nucleon which moves from state i to state f is given by the Hamiltonian $H_{\pi NN}$, while the various parts of the vertex operator j_π^α have simple physical interpretations. The δ-function reflects a locality of the interaction; the pion can only be emitted from a nucleon located at $\underset{\sim}{x}_1$. The pion has spin 0 and negative parity. Because parity is conserved in the strong interactions, the vertex must include a compensating negative-parity operator, and only $\vec{\nabla}$ (the pion's momentum operator) is available, because we have ruled out the nucleon's momentum (we are working in the static limit). The vertex must be Hermitian and a scalar and the only other vector available is $\vec{\sigma}(1)$, the nucleon's spin. Alternatively, eqn. (23) reflects the pion's preferred p-wave interaction with a nucleon. The nucleon isospin operator $\tau^\alpha(1)$ allows $H_{\pi NN}$ to be an isospin scalar of the form $\vec{\tau}\cdot\vec{\phi}_\pi$ or $\tau^\alpha\phi_\pi^\alpha$. The dimensionless coupling constant f ($f_0^2 \equiv f^2/4\pi \cong 0.079$) determines the strength of the interaction and the (-) sign is conventional. We see that the <u>static</u> j_π^α is uniquely determined by invariance (spin, parity, isospin) arguments.

The other bit of physics we require is the equation of motion of the pion field, which allows us to propagate a pion from one point to another, or, equivalently, to "tie together" two vertices. This equation for the pion field is the usual wave equation for massive particles, and mirrors the analogous Maxwell equation for the electromagnetic vector potential:

$$(\vec{\nabla}^2-\mu^2-\frac{\partial^2}{\partial t^2})\;\phi_\pi^\alpha(x) = j_\pi^\alpha(x) \quad , \tag{24}$$

where we have allowed for finite propagation time of the pion. This violates our static assumption and we should neglect all time dependence, resulting in

$$(\vec{\nabla}^2-\mu^2)\phi_\pi^\alpha(\underset{\sim}{x}) = j_\pi^\alpha(\underset{\sim}{x}) \quad , \tag{25}$$

which can be solved for $\phi_\pi^\alpha(\underset{\sim}{x})$:

$$\phi_\pi^\alpha(\underset{\sim}{x}) = \frac{-1}{4\pi}\int h_o(|\underset{\sim}{x}-\underset{\sim}{y}|)J_\pi^\alpha(\underset{\sim}{y})\ d^3y = \frac{f}{4\pi\mu}\ \tau^\alpha(1)\ \vec{\sigma}(1)\cdot\vec{\nabla}_1 h_o(|\underset{\sim}{x}-\underset{\sim}{x}_1|), \tag{26}$$

where the static pion propagator is

$$h_o(z) = \frac{e^{-\mu z}}{z} \quad . \tag{27}$$

The integrated energy shift due to the exchange of a pion being omitted by nucleon 1 at $\vec{y}$ and absorbed by nucleon 2 at $\vec{x}$ is then simply given by perturbation theory:

$$\Delta E = \int j_\pi^\alpha(\underset{\sim}{x})\phi_\pi^\alpha(\underset{\sim}{x})d^3x = \frac{-1}{4\pi}\int\int\ j_\pi^\alpha(\underset{\sim}{x})h_o(|\underset{\sim}{x}-\underset{\sim}{y}|)j_\pi^\alpha(\underset{\sim}{y})\ d^3xd^3y \quad . \tag{28}$$

In this exercise we have ignored the nucleon wave functions (ψ) in eqn. (22) because we are constructing an operator in the Hilbert space of the nucleons. Identifying ΔE as the OPE potential, $V_\pi(\underset{\sim}{r})$, we obtain after performing the integrals,

$$V_\pi(\underset{\sim}{r}) = \frac{f_o^2}{\mu^2}\ (\vec{\tau}(1)\cdot\vec{\tau}(2))\ \vec{\sigma}(1)\cdot\vec{\nabla}\ \vec{\sigma}(2)\cdot\vec{\nabla}h_o(r) \quad , \tag{29}$$

where $\vec{r} = \vec{x}_1-\vec{x}_2$. The isospin dependence is explicit and is responsible for exchange currents, as we indicated earlier. Moreover, the derivatives lead to the extremely important tensor force.

The model-independent pion electromagnetic interactions are also easily obtained. Typically, the electromagnetic interaction vertices can be obtained by means of the "minimal" substitution: all factors of momentum, $\vec{p}$, in the strong interaction Hamiltonian are replaced by $(\vec{p}-e\vec{A})$, where $\vec{A}$ is the electromagnetic vector potential and e is the fundamental charge. Indeed, this is the origin of the nucleon convection current via the kinetic energy, T. We also note that the magnetization current is special (it is solenoidal, or divergenceless), and does not follow from such arguments. In eqns. (22) and (23) we

resort to a trick and write

$\vec{\nabla}_1\vec{\phi}_\pi(\underset{\sim}{x}_1)\cdot\vec{\tau}(1)$ as $i[\vec{p}_1,\vec{\tau}(1)\cdot\vec{\phi}_\pi(\underset{\sim}{x}_1)]$, replace $\vec{p}_1$ by $\vec{p}_1-e_1\vec{A}_1$,

and use the isospin form of e_1, which leads to

$$H_{\gamma\pi N} = -e\int\psi_f^\dagger(\underset{\sim}{x})\hat{\vec{J}}_{SG}(\underset{\sim}{x})\psi_i(\underset{\sim}{x})\cdot\vec{A}(\underset{\sim}{x})\ d^3x \quad , \tag{30}$$

where

$$\hat{\vec{J}}_{SG}(\underset{\sim}{x}) = \frac{-f}{\mu}\vec{\sigma}(1)\delta^3(\underset{\sim}{x}-\underset{\sim}{x}_1)(\vec{\tau}(1)\times\vec{\phi}_\pi)_z \quad , \tag{31}$$

and we have used $[\tau_z,\ \vec{\tau}\cdot\vec{\phi}_\pi] = -2i(\vec{\tau}\times\vec{\phi}_\pi)_z$. The electromagnetic current operator corresponding to fig. 19b can now be easily calculated in perturbation theory using eqn. (26):

$$\Delta E = -e\int\vec{J}_{SG}(\underset{\sim}{x})\cdot\vec{A}(\underset{\sim}{x})\ d^3x \quad , \tag{32}$$

where

$$\vec{J}_{SG}(\underset{\sim}{x}) = \frac{f_o^2}{\mu^2}\vec{\sigma}(1)\delta^3(\underset{\sim}{x}-\underset{\sim}{x}_1)\vec{\sigma}(2)\cdot\vec{\nabla}_x h_o(\underset{\sim}{x}-\underset{\sim}{x}_2)(\vec{\tau}(1)\times\vec{\tau}(2))_z + (1\leftrightarrow 2) \tag{33}$$

This result is quite obvious, given eqn. (31) and our previous derivation for OPEP; we simply replaced ϕ_π^α in eqn. (31) by that in eqn. (26). There are <u>two</u> terms, because the process is not symmetrical in nucleons 1 and 2, unlike the OPEP case.

The remaining model-independent process is depicted in fig. (19c), where the fundamental pion electromagnetic vertex is given by

$$H_{\gamma\pi\gamma} = e\int[\phi_{\underset{\sim}{\pi}}^\dagger(\underset{\sim}{x})\times\overleftrightarrow{\nabla}_x\phi_{\underset{\sim}{\pi}}(\underset{\sim}{x})]_z\cdot\vec{A}(\underset{\sim}{x})\ d^3x \quad , \tag{34}$$

where $f\overleftrightarrow{\nabla}g \equiv f\vec{\nabla}g - g\vec{\nabla}f$. Up to a sign, the form is almost obvious, since the nucleon convection current is often written in the form: $(\psi_f^\dagger\vec{p}\psi_i + (\vec{p}\psi_f)^\dagger\psi_i)/2M$. The unusual aspect is the isospin dependence, which has been constructed[51] to give a (+) sign for the π^+ interaction, a (-) sign for the π^- interaction, and 0 for a π^o.

The true-exchange current is obtained by connecting <u>either</u> $\phi_{\underset{\sim}{\pi}}$ ($\equiv \vec{\phi}_\pi$) to nucleon 1 and the other one to nucleon 2; because the interaction is symmetric in 1 and 2, we don't double count this way. We find

$$\vec{J}_{ex}(\underset{\sim}{x}) = \frac{-f_o^2}{\mu^2}(\vec{\tau}(1)\times\vec{\tau}(2))_z\vec{\sigma}(1)\cdot\vec{\nabla}_x h_o(|\underset{\sim}{x}-\underset{\sim}{x}_1|)\overleftrightarrow{\nabla}_x\vec{\sigma}(2)\cdot\vec{\nabla}_x h_o(|\underset{\sim}{x}-\underset{\sim}{x}_2|), \tag{35}$$

which has the same isospin structure as $\vec{J}_{SG}(\underset{\sim}{x})$. We also note that this process is semiclassical[51].

The remaining contribution is fig. 19d. Because of its complexity, and the fact that it is model dependent, our derivation will be somewhat schematic. The Δ-isobar is a nucleon excited state with spin and isospin 3/2 and positive parity, which we treat as a static particle. The interaction depicted in fig. 19d corresponds to the electromagnetic creation of the isobar and its subsequent decay by pion emission. We have not shown the additional process with the opposite time ordering, the electromagnetic interaction occurring last. The transition from $1/2^+$ to $3/2^+$ can be magnetic dipole or electric quadrupole, the latter being negligible. Current operators for magnetic dipole processes have the form

$\vec{J}_\Delta(\underset{\sim}{x}) = \vec{\nabla}_x\times\vec{M}_\Delta(\underset{\sim}{x})$, or $H_{\Delta N\gamma} = -e\int\vec{M}_\Delta(\underset{\sim}{x})\cdot\vec{B}(\underset{\sim}{x})d^3x$, where $\vec{B}$ is the magnetic field. Assuming that the electromagnetic interaction occurs on nucleon 1, the basic process is represented in second-order perturbation theory by

$$\vec{M}_\Delta(\underset{\sim}{x}) = \frac{-f\mu_v}{2\mu M}\sum_{M_\Delta}\frac{\langle\frac{1}{2}M'|\vec{S}_\Delta^\alpha\cdot\vec{\nabla}_1\phi_\pi^\alpha(\underset{\sim}{x}_1)|3/2\ 3/2M_\Delta\rangle\langle 3/2\ 3/2M_\Delta|\hat{\vec{\mu}}_\Delta\delta^3(\underset{\sim}{x}-\underset{\sim}{x}_1)|\frac{1}{2}M\rangle}{-\Delta M}, \tag{36}$$

where we have written the effective ($\pi N\Delta$)-vertex as $-(f/\mu)\vec{S}_\Delta^\alpha\cdot\vec{\nabla}_1\phi_\pi^\alpha(\underset{\sim}{x}_1)$ in complete analogy with eqn. (22) ($\vec{S}_\Delta^\alpha$ is the NΔ transition-"spin" operator, which replaces $\vec{\sigma}_1$ in eqn. (23)), the magnetic dipole <u>isovector</u> ($\gamma N\Delta$)-vertex as $\mu_v\hat{\vec{\mu}}_\Delta\delta^3(\underset{\sim}{x}-\underset{\sim}{x}_1)/2M$ in analogy with eqn. (20), and the energy denominator is simply the negative of the Δ-nucleon mass difference, $-\Delta M = -300$ MeV. The only complexity in eqn. (36) is the

intermediate-state spin sum over the magnetic quantum numbers of both spin and isospin (M_Δ), which produces projection operators in the nucleon spin and isospin space. We give these without proof; the spin-projection operators for spin 1/2 or 3/2 intermediate states are:

$$\sum_{M_I} \langle \tfrac{1}{2}M'|\vec{A}_o\cdot\vec{V}|JM_I\rangle\langle JM_I|\vec{B}_o\cdot\vec{V}'|\tfrac{1}{2}M\rangle$$

$$\equiv \langle \tfrac{1}{2}M'|\hat{P}_J|\tfrac{1}{2}M\rangle\langle \tfrac{1}{2}\tfrac{1}{2}|V_z|J\tfrac{1}{2}\rangle\langle J\tfrac{1}{2}|V_z'|\tfrac{1}{2}\tfrac{1}{2}\rangle \quad , \tag{37}$$

where $\vec{A}_o$ and $\vec{B}_o$ are constant vectors,

$$\hat{P}_{1/2} = \vec{A}_o\cdot\vec{B}_o + i\vec{\sigma}\cdot\vec{A}_o\times\vec{B}_o \quad , \tag{38}$$

$$\hat{P}_{3/2} = \vec{A}_o\cdot\vec{B}_o - i\vec{\sigma}\cdot\vec{A}_o\times\vec{B}_o/2 \quad , \tag{39}$$

$\vec{V}$ and $\vec{V}'$ are any (vector) nuclear operators and $\vec{\sigma}$ is the nucleon spin operator. The isospin projection is analogous with $\vec{\sigma}\to\vec{\tau}$. The derivation is best performed using the Wigner-Eckart theorem in a brute-force manner.

We can now easily complete the derivation, using eqn. (39). The second time ordering, not shown in fig. (19), is equivalent to the Hermitian conjugate of eqn. (36). Using this we find

$$\vec{J}_\Delta(\underset{\sim}{x}) = \frac{\lambda\mu_v f_o^2}{4M\mu^2\Delta M}\vec{\nabla}\times\{\delta^3(\underset{\sim}{x}-\underset{\sim}{x}_1)[(\vec{\tau}(1)\times\vec{\tau}(2))_z\vec{\sigma}(1)\times\vec{\nabla}_x - 4\tau_z(2)\vec{\nabla}_x]\vec{\sigma}(2)$$

$$\cdot\vec{\nabla}_x h_o(\underset{\sim}{x}-\underset{\sim}{x}_2)+(1\leftrightarrow 2)\} \quad , \tag{40}$$

where

$$\lambda = \langle \tfrac{1}{2}\tfrac{1}{2}|\hat{S}_\Delta^{zz}|3/2\ \tfrac{1}{2}\rangle\langle 3/2\ \tfrac{1}{2}|\hat{\mu}_\Delta^z|\tfrac{1}{2}\tfrac{1}{2}\rangle \tag{41}$$

is calculated for a proton (isospin component $+\frac{1}{2}$) with spin component $+\frac{1}{2}$, using the z-component in both spin and isospin for the operators $\hat{\vec{S}}^\alpha$ and $\hat{\vec{\mu}}_\Delta$. Equation (40) is model independent in the sense that only

angular momentum arguments have been used in its construction. The operators $\hat{S}^{\alpha}_{\Delta}$ and $\hat{\mu}_{\Delta}$ were defined so that they are dimensionless, as is λ, which contains all of the model dependence. If we resort to the quark model for the nucleon and isobar, we find

$$\lambda^{QM} = \frac{16}{25} \quad , \tag{42}$$

while the Chew-Low model of the isobar[52] gives

$$\lambda^{CL} = \frac{4}{5} \quad . \tag{43}$$

Deriving eqn. (42) is an excellent exercise (hint: $\langle \hat{S}^{zz}_{\Delta} \rangle = 4\sqrt{2}/5$; $\langle \hat{\mu}^{z}_{\Delta} \rangle = 2\sqrt{2}/5$).

This completes our derivation of the pion-exchange currents. The final result is

$$\vec{J}_{\pi}(\underset{\sim}{x}) = \vec{J}_{SG}(\underset{\sim}{x}) + \vec{J}_{ex}(\underset{\sim}{x}) + \vec{J}_{\Delta}(\underset{\sim}{x}) \quad . \tag{44}$$

Another very good exercise is to verify that eqn. (21) holds for $\vec{J}_{\pi}$, with H replaced by OPEP.

D. Evidence for Exchange Currents

Most of the evidence for exchange currents centers on magnetic dipole processes, and in particular on static and transition magnetic moments. We have already mentioned[27] the isovector magnetic transition between the $^3S_1$ deuteron and the $^1S_0$ threshold state of the np system. What about the deuteron magnetic moment? Because the deuteron ground state is an isoscalar system, the (isovector) exchange currents we derived earlier do not contribute. The currents due to the exchange of positive and negative mesons <u>exactly</u> cancel; this is precisely the meaning of isoscalar. Only those exchange currents of (relativistic) order $(1/c^3)$ and higher contribute. Indeed, the deuteron magnetic moment is usually written[21] in the form

$$\mu_d = \mu_s^o - \tfrac{3}{2}P(D)(\mu_s^o - \tfrac{1}{2}) + \Delta\mu_d = .85774 \quad , \tag{45}$$

where the numerical value is experimental, P(D) is the deuteron d-state probability and $\Delta\mu_d$ is the contribution from small relativistic corrections of various types. It is worth noting that relativistic corrections have an intrinsic ambiguity built into them; different methods for calculating them give different operators. This doesn't mean that observables, or matrix elements of these operators, are ambiguous. They are not, because the same ambiguities are contained in the nuclear potentials and the wavefunctions, and exactly cancel those in the operator. The ambiguity is therefore nothing more than a unitary transformation. It causes a complication in eqn. (45), however, since both P(D) and $\Delta\mu_d$ are affected by it, although the ambiguity in both terms can be shown to cancel[21]. It does make it impossible to attribute any fundamental meaning to P(D); that is, it is not measurable, and the division between the second and third terms in eqn. (45) is artificial. Nevertheless, the scale of the corrections $(\mu_d-\mu_s^\circ)/\mu_s^\circ$ is -.0251, and P(D)=3.9% satisfies eqn. (45) if we arbitrarily set $\Delta\mu_d$ to zero.

The trinucleons have isospin ½, so that the magnetic moments can be broken down into an isoscalar component ($\mu_s=\mu(^3He)+\mu(^3H)$) similar to the deuteron case, and an isovector component ($\mu_v=\mu(^3He)-\mu(^3H)$). One finds that[53]

$$\mu_s = \mu_s^\circ - 2P_D(\mu_s^\circ-\tfrac{1}{2}) + \Delta\mu_s = 0.85131 \quad , \tag{46}$$

and

$$\mu_v = -\mu_v^\circ[1-\tfrac{4}{3}P_S'-\tfrac{2}{3}P_D]+\Delta\mu_o+\Delta\mu_v = -5.10641 \quad , \tag{47}$$

where $\Delta\mu_o$ is a very small contribution from orbital angular momentum, and $\Delta\mu_s$ and $\Delta\mu_v$ represent corrections to the impulse approximation. The isoscalar part is nearly identical to the deuteron case, and P_D=3.8% produces equality between impulse approximation and experiment, when $\Delta\mu_s$ vanishes. The isovector case is rather different. Using reasonable values of P_S'=1% and P_D=10% produces $\Delta\mu_v/\mu_v^\circ$=-16.5%, compared to $\Delta\mu_s/\mu_s^\circ$= 5.4%. The scale of the two corrections is different, as is the sign.

The isoscalar discrepancy is consistent with a (large) correction of relativistic order, while the isovector case is much larger, and is indicative of nonrelativistic exchange currents. Note that the absolute size of $\Delta\mu_v$ would be comparable to the size of the impulse approximation, were μ_v^o equal to 1, which is consistent with our previously discussed rules of scale for exchange currents. The size of the seagull part of the pion-exchange current is typically $\Delta\mu_v^{SG}/\mu_v^o \cong$ -(14-15)%, or most of the discrepancy. The true-exchange and isobar parts of the pionic current have opposite signs and typical values $\Delta\mu_v/\mu_v^o \cong \pm 2\%$, with the upper and lower signs referring to the true-exchange and isobar contributions, respectively. The net theoretical result is slightly too small, but dramatically illustrates the importance of pion-exchange currents.

The analysis of the tritium β-decay matrix element is identical to that of the isovector magnetic moment in impulse approximation. The nuclear matrix elements are $(1+3g_A^2M_A^2)$, where the superallowed Fermi part is 1, g_A is the axial vector coupling constant, and the Gamow-Teller matrix element has the form

$$|M_A| = 1 - \frac{4}{3}P_S' - \frac{2}{3}P_D + \Delta M_A = 1 - 0.042(8) \quad , \tag{48}$$

where the numerical value is experimental.[54] Using our previous estimate of probabilities we estimate[2] $\Delta M_A = 0.04(2)$. The size of this correction is consistent with a relativistic correction and our previous analysis that the impulse approximation axial vector current is class II, and has no nonrelativistic exchange currents.

Given the fact that the magnetic moments are very strongly affected by pion-exchange currents, we should also expect that the magnetic form factor, or Fourier transform of the magnetization density, is similarly affected. This is indicated for ^{3}He in fig. 20 which shows three calculations by Hajduk, Sauer, and Strueve[39], together with the data. The shape of $|F_{mag}|$ as a function of the momentum transfer, q, is a typical diffraction structure. The impulse approximation (no exchange currents) based on the Paris potential has its diffraction minimum at much too small a value of q. Including the

exchange currents (labelled isobar model) moves the diffraction minimum out toward the experimental results. Unfortunately, theoretical uncertainties in how to deal with the nucleon form factors (the large dots in fig. (19)) in the exchange currents lead to (at least) three different prescriptions, two of which are indicated in the figure (labelled F_1 and G_E).

The problem is seen most clearly in the charge form factor, which in impulse approximation has the structure

$$F_B(q^2) = \int d^3r\, e^{i\underline{q}\cdot\underline{r}} \rho_0(\underline{r}) \quad . \tag{49}$$

The subscript "B" indicates that this is the "body" form factor, the probability that, when one nucleon is struck and receives momentum q, the recoiling nucleus is capable of reconstituting itself in the ground state. That probability is rather small, because small momentum components, rather than large, are most probable in a nucleus, which is why form factors are always shown on semi-log plots! The most probable reaction is for the struck nucleon to be ejected. But in "grabbing" the nucleus the electromagnetic interaction must first grab a nucleon, and that does not have unit probability, but rather $G_N(q^2)(\leq 1)$, because the nucleon has its own structure. In accordance with accepted probability practice one takes the product of the probability distributions:

$$F_{ch}(q^2) = G_N(q^2)F_B(q^2) \quad . \tag{50}$$

In dealing with the pion-seagull exchange current, it is not known which type of nucleon form factor, G_N, to use, the electric (charge) form factors[48] F_1 or G_E, or the axial vector form factor, G_A. Experiment would appear to prefer F_1 or G_A (both are larger than G_E), but the calculations are not sufficiently unambiguous to allow that conclusion.

Similar results are evident in the ^3H magnetic form factor together with new high momentum transfer data eagerly awaited for two decades[55]. The dashed curve is the impulse approximation and the

solid curve includes a variety of exchange currents. The agreement between theory and experiment is rather good.

Just as long-standing discrepancies between theory and experiment involving thermal np radiative capture pointed to exchange currents, so did problems with thermal nd radiative capture ($n+d \to {}^3H+\gamma$). In the latter case, the capture rate vanishes in impulse approximation if one assumes that all the forces between nucleons are identical. In that limit the (s-wave) ground state wavefunction is an eigenfunction of the magnetic moment operator, and the matrix element vanishes by orthogonality. This greatly suppresses the doublet part of the decay rate, which we see from eqns. (46) and (47) if we drop the leading order μ_s^o- and μ_v^o-terms. The remaining probabilities are now the overlaps of the appropriate pieces of the two wavefunctions. In addition the decay can also proceed from the quartet part of the nd state. Recent measurements of the total rate summarized in ref. 2 give a cross-section of .515(9) mb, 600 times small than the corresponding np case.

Extensive calculations by Torre and Goulard[56] have established that in impulse approximation the quartet rate is 20 percent larger than the doublet. The exchange currents lower the former by 20 percent while raising the latter by 500 percent, increasing the impulse approximation result of .2 mb to a total of .6 mb, in fairly good agreement with experiment. The seagull, isobar and true-exchange pionic currents contribute roughly in the ratio 3:2:-1.

We have concentrated almost entirely on the long-range pionic currents, motivated by the shape of the correlation function. Is this adequate? There are a wide variety of short-range contributions, most of which can be obtained from fig. 19 by replacing a pion propagator by that of a heavy meson. Typically these contributions are 10-20 percent of the pionic ones, at least for small momentum transfers, and their calculation is much more model dependent.

Finally, we show the charge form factors[55] of ^3He and ^3H in figs. 22 and 23, together with the calculations of Hajduk, Sauer, and Strueve[39]. The impulse approximation and the HS isobar model for ^3He are deficient in the region of the secondary diffraction maximum. The addition of ambiguous exchange currents of relativistic order improves

the agreement. Unfortunately the "realistic" potential models which are used to calculate wave functions don't have the correct form to accommodate relativistic corrections, and the cancellations which must take place to eliminate the ambiguity from matrix elements cannot take place. The results for ^3H are shown together with two calculations using different (nonstatic) models of the π-nucleon vertex (PS and PV). This model dependence partially reflects the ambiguity discussed above. This is a murky and technically complex subject, which the interested reader can find discussed elsewhere[26].

E. Summary

We summarize by noting that in isovector magnetic dipole processes, pion-exchange currents can make sizeable contributions. Contributions from heavy-meson exchange are smaller, because nucleons don't like to overlap at small separations. The dominant meson-exchange effects occur in the isovector current operator, while small (ambiguous) contributions can occur to the charge, isoscalar current, and axial vector current operators.

IV. ACKNOWLEDGEMENTS

This work was performed under the auspices of the U. S. Department of Energy. The author would like to thank his collaborators, G. L. Payne, B. F. Gibson, C. R. Chen, and E. L. Tomusiak, for their assistance in preparing the lectures.

FIGURE CAPTIONS

Figure 1. Jacobi coordinates (x_1,y_1,θ_1) for trinucleon problem.

Figure 2. Comparison of centrifugal kinetic energy with the MT-V potential (top) and partial-wave projected triton correlation functions for that potential (bottom).

Figure 3. Configuration space regions for Nd scattering problem.

Figure 4. Faddeev wavefunction for quartet nd scattering, ψ_1, plotted versus x and y.

Figure 5. Schrödinger wavefunction component, v_3, for $\theta=0°$ generated from ψ_1 in fig. 4, plotted versus x and y.

Figure 6. The function at the top is approximated by the sum of 5 spline functions in the middle. The use of such splines with a second-order differential equation leads to the banded matrix shown at the bottom.

Figure 7. Schematic trinucleons with identical forces betweer protons (shaded) and neutrons in (a) and with different forces for ^{3}He in (b) and ^{3}H in (c).

Figure 8. Calculated trinucleon (point nucleon) rms charge radii decomposed into isoscalar (s) and difference (v) contributions in impulse approximation, together with data, plotted versus corresponding binding energy. The ^{3}He calculations contained no Coulomb force.

Figure 9. Calculated trinucleon S′-state percentages plotted versus corresponding binding energy.

Figure 10. Calculated trinucleon (point nucleon) rms charge radii in impulse approximation, plotted versus corresponding binding energy. The ^{3}He calculations contained no Coulomb force.

Figure 11. ^{3}He Coulomb energy, E_c, plotted versus the corresponding hyperspherical approximation, E_c^H.

Figure 12. Various physical processes contributing to three-nucleon forces. Solid, dashed, shaded and double lines depict nucleons, pions, isobars (nucleon excited states), and heavy mesons, respectively.

Figure 13. Experimental (x's) and theoretical charge densities for ^{3}He. The theoretical curves correspond to including or not including a Coulomb force between the protons in ^{3}He.

Figure 14. The spatially symmetric (S-state) component, u, of the Schrödinger wave function from a 5-channel RSC calculation for $\theta=0°$, plotted versus x and y.

Figure 15. The Faddeev wave function component, ψ_1^S, which generated u in fig. 14, plotted versus x and y.

Figure 16. Doublet nd and pd scattering lengths plotted versus ^{3}H and ^{3}He binding energies, respectively. Individual points are from theoretical calculations (triangles, squares, and circles correspond to realistic two-body force models, the additional inclusion of three-body forces, and unrealistic two-body force models).

Figure 17. Scenario for probing three-nucleon forces with pd initial state (a) becoming equilateral (b) and collinear (c) three-body breakup configurations.

Figure 18. Two-body triton (isoscalar) correlation functions for the RSC and AV14 potential models, together with the ranges of various meson exchanges.

Figure 19. One-pion-exchange processes contributing to OPEP in (a), and to the OPE currents in (b)-(d).

Figure 20. ^{3}He magnetic form factor, together with 3 calculations by Hadjuk, Sauer, and Strueve.

Figure 21. ^{3}H magnetic form factor, together with 2 calculations by Hadjuk, Sauer, and Strueve.

Figure 22. ^{3}He charge form factor, together with 3 calculations by Hajduk, Sauer, and Strueve.

Figure 23. ^{3}H charge form factor, together with 2 calculations by Hajduk, Sauer, and Strueve.

REFERENCES

1) Bethe, H. A. and Bacher, R. F., Rev. Mod. Phys. 8, 82 (1936).
2) Friar, J. L., Gibson, B. F., and Payne, G. L., Ann. Rev. Nucl. Part. Sci. 34, 403 (1984).
3) Payne, G. L., Friar, J. L., Gibson, B. F., and Afnan, I. R., Phys. Rev. C 22, 823 (1980).
4) Friar, J. L., Tomusiak, E. L., Gibson, B. F., and Payne, G. L., Phys. Rev. C 24, 677 (1981).
5) Malfliet, R. A. and Tjon, J. A., Nucl. Phys. A127, 161 (1969).
6) Foldy, L. L. and Tobocman, W., Phys. Rev. 105, 1099 (1957).
7) Glöckle, W., Nucl. Phys. A141, 620 (1970).
8) Payne, G. L., Klink, W. H., Polyzou, W. N., Friar, J. L., and Gibson, B. F., Phys. Rev. C 30, 1132 (1984).
9) Faddeev, L. D., Zh. Eksp. Teor. Fiz. 39, 1459 (1960).
10) Noyes, H. P., in "Three Body Problem in Nuclear and Particle Physics," edited by J. S. C. McKee and P. M. Rolph (North-Holland, Amsterdam, 1970), p. 2.
11) Glöckle, W., Z. Phys. 271, 31 (1974).
12) Prenter, P. M., "Splines and Variational Methods" (Wiley, New York, 1975).
13) De Boor, C. and Swartz, B., SIAM (J. Num. Anal.) 10, 582 (1973).
14) Chen, C. R., Payne, G. L., Friar, J. L., and Gibson, B. F., Phys. Rev. C 31, 2266 (1985).
15) Reid, R. V., Jr., Ann. Phys. (N. Y.) 50, 411 (1968).
16) Wiringa, R. B., Smith, R. A., Ainsworth, T. A., Phys. Rev. C 29, 1207 (1984).
17) de Tourreil, R. and Sprung, D. W. L., Nucl. Phys. A201, 193 (1973).
18) LaCombe, M., Loiseau, B., Richard, J. M., Vinh Mau, R., Côte, J., et al., Phys. Rev. C 21, 861 (1980).
19) Hajduk, C. and Sauer, P. U., Nucl. Phys. A369, 321 (1981).
20) Friar, J. L., Gibson, B. F., Chen, C. R., and Payne, G. L., Phys. Lett. (to appear).
21) Friar, J. L., Phys. Rev. C 20, 325 (1979).

22) Friar, J. L. and Gibson, B. F., Phys. Rev. C 18, 908 (1978).

23) Payne, G. L., Friar, J. L., and Gibson, B. F., Phys. Rev. C 22, 832 (1980).

24) Friar, J. L., Nucl. Phys. A156, 43 (1970); Fabre de la Ripelle, M., Fizica 4, 1 (1972).

25) Kalos, M. H., Phys. Rev. 128, 1791 (1962).

26) Friar, J. L., Gibson, B. F., and Payne, G. L., Phys. Rev. C 30, 441 (1984)

27) Riska, D. O. and Brown, G. E., Phys. Lett. 38B, 193 (1972).

28) Olsson, M. G., Osypowski, E. T., and Monsay, E. H., Phys. Rev. D17, 2938 (1978).

29) Siegert, A. J. F., Phys. Rev. 52, 787 (1937).

30) Kirk, J., private communication, points out that the inclination of the satellite orbit is changed in a significant (though very small) way by the tides. Computer codes which accurately calculate satellite motion must include this effect.

31) Axilrod, B. M. and Teller, E., J. Chem. Phys. 11, 299 (1943).

32) Bell, R. J. and Zucker, I. J., in "Rare Gas Solids, Vol. I", ed. by M. L. Klein and J. A. Venables (Academic Press, London, 1976), p. 122. The effects of three-atom forces are rather important in rare gas solids.

33) Friar, J. L. and Coon, S. A., Phys. Rev. C (to be published).

34) Primakoff, H. and Holstein, T., Phys. Rev. 55, 1218 (1939).

35) Coon, S. A., Scadron, M. D., McNamee, P. C., Barrett, B. R., Blatt, D. W. E., and McKellar, B. H. J., Nucl. Phys. A317, 242 (1979).

36) Coelho, H. T., Das, T. K., and Robilotta, M. R., Phys. Rev. C 28, 1812 (1983).

37) Carlson, J., Pandharipande, V. R., and Wiringa, R. B., Nucl. Phys. A401, 59 (1983).

38) Hajduk, C. and Sauer, P. U., Nucl. Phys. A322, 329 (1979).

39) Hajduk, C., Sauer, P. U., and Strueve, W., Nucl. Phys. A405, 581 (1983).

40) Friar, J. L., Gibson, B. F., Tomusiak, E. L., and Payne, G. L., Phys. Rev. C 24, 665 (1981).

41) Friar, J. L., Gibson, B. F., Payne, G. L., and Chen, C. R., Phys. Rev. C 30, 1121 (1984); and to be published.

42) Phillips, A. C., Rep. Prog. Phys. 40, 905 (1977).

43) Slaus, I., Akaishi, Y., and Tanaka, H., Phys. Rev. Lett. 48, 993 (1982).

44) Bömelburg, A., Glöckle, W., and Meier, W., in "Few Body Problems in Physics," Vol. II, ed. by B. Zeitnitz (North-Holland, Amsterdam, 1984), p. 483.

45) Chen, C. R., Payne, G. L., Friar, J. L., and Gibson, B. F., Phys. Rev. Lett. (to appear).

46) Wiringa, R. B., Friar, J. L., Gibson, B. F., Payne, G. L., and Chen, C. R., Phys. Lett. 143B, 273 (1984).

47) Friar, J. L., AIP Conference Proceedings 97, 378 (1983).

48) Friar, J. L., in "Electron and Pion Interactions with Nuclei at Intermediate Energies," W. Bertozzi, S. Costa, and C. Schaerf, eds., (Harwood, N. Y., 1980), p. 143.

49) Friar, J. L., Phys. Rev. C 27, 2078 (1983).

50) Campbell, D. K., in "Heavy Ions and Mesons in Nuclear Physics," Les Houches, Course XXX, R. Balian, ed. (North Holland, Amsterdam, 1977), p. 553, is an excellent introduction to this topic.

51) Friar, J. L., Tomusiak, E. L., and Dubach, J., Phys. Rev. C 25, 1659 (1982).

52) Thakur, J. and Foldy, L. L., Phys. Rev. C8, 1957 (1973), contains an excellent discussion of these results, with references to previous work.

53) Tomusiak, E. L., Kimura, M., Friar, J. L., Gibson, B. F., Payne, G. L., and Dubach, J., submitted to Phys. Rev. C.

54) Bargholtz, C., Phys. Lett. 112B, 193 (1982).

55) F. P. Juster, et. al., contributed paper at conference "Nuclear Physics with Electromagnetic Probes," (Paris, July 1-5, 1985), p. 156.

56) Torre, J. and Goulard, B., Phys. Rev. C 28, 529 (1983).

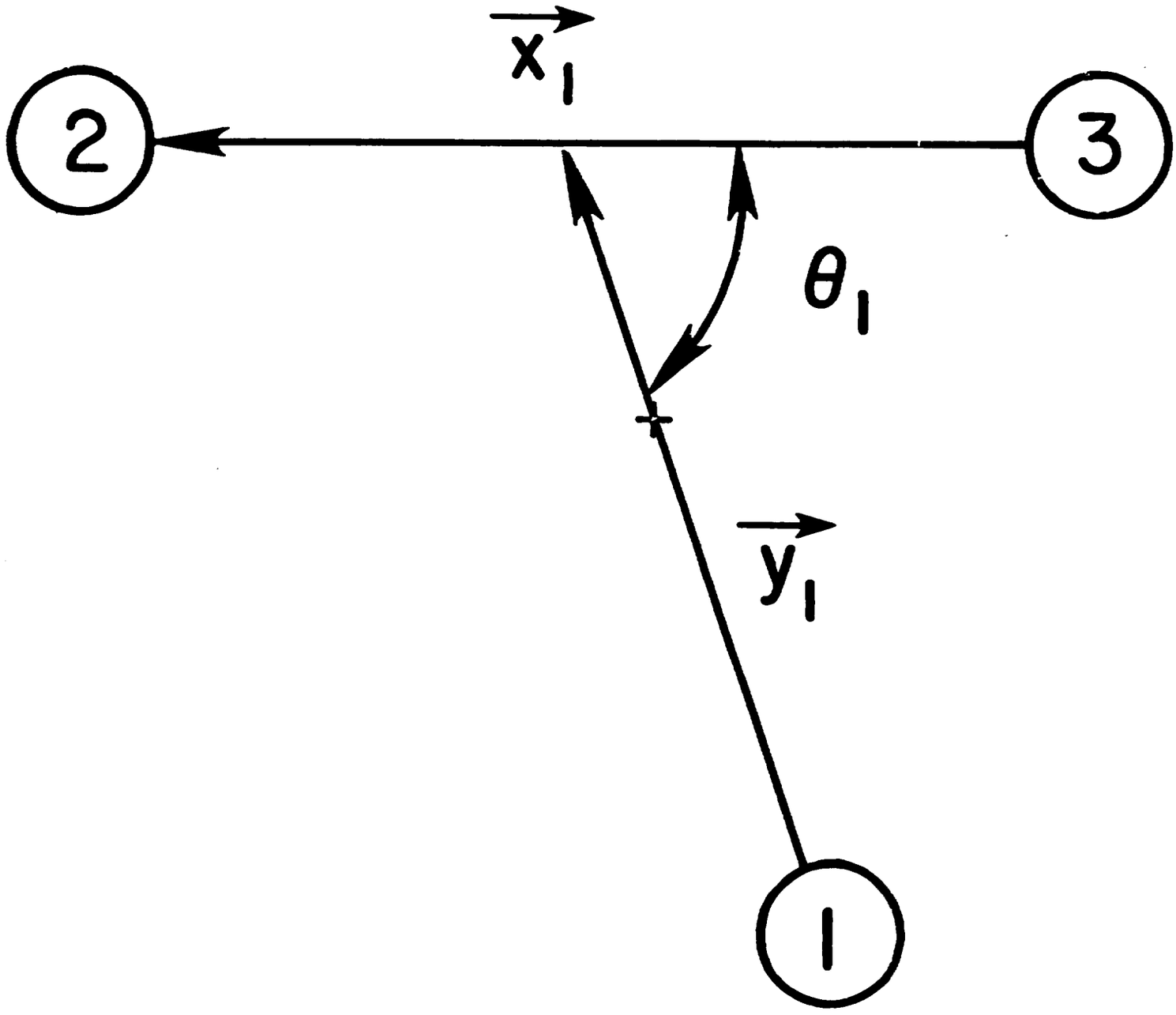
$\vec{x}_1$
2
3
θ_1
$\vec{y}_1$
1

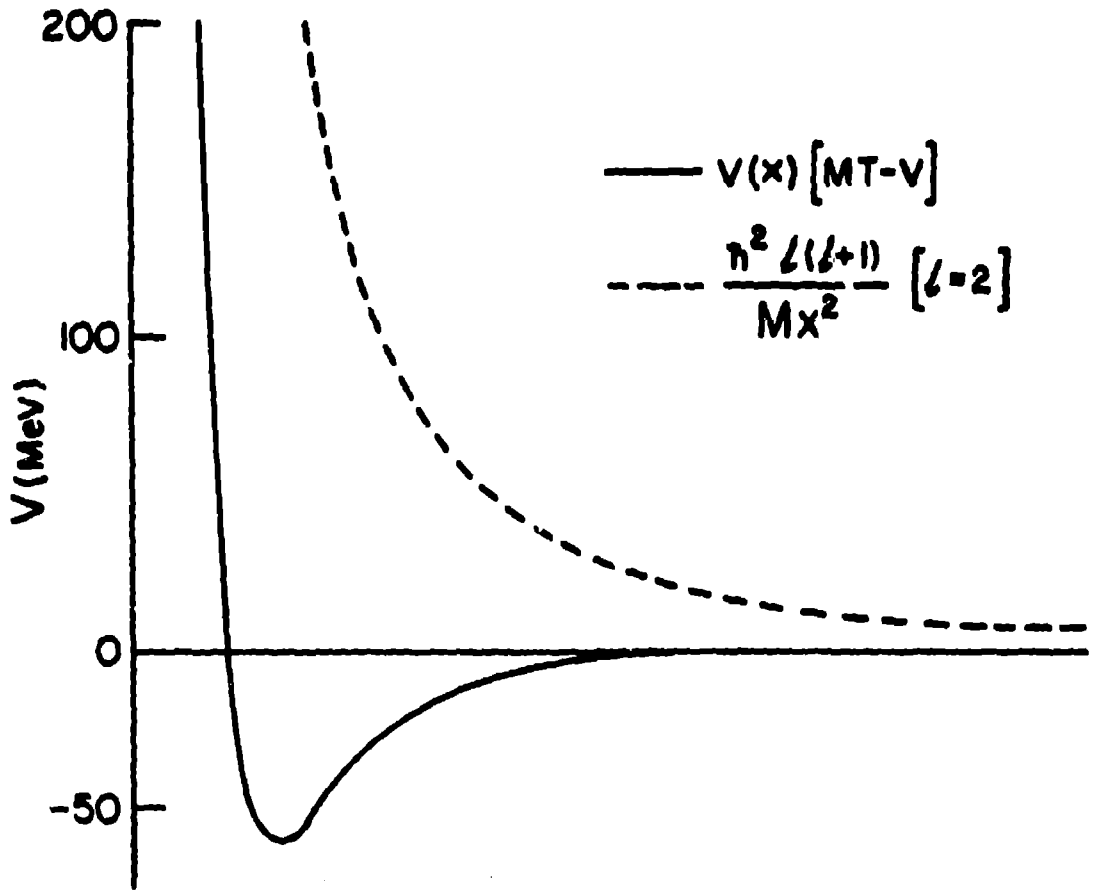
200
100
0
-50
V(MeV)
V(x) [MT-V]
$\frac{\hbar^2 \ell(\ell+1)}{Mx^2}$ [ℓ=2]

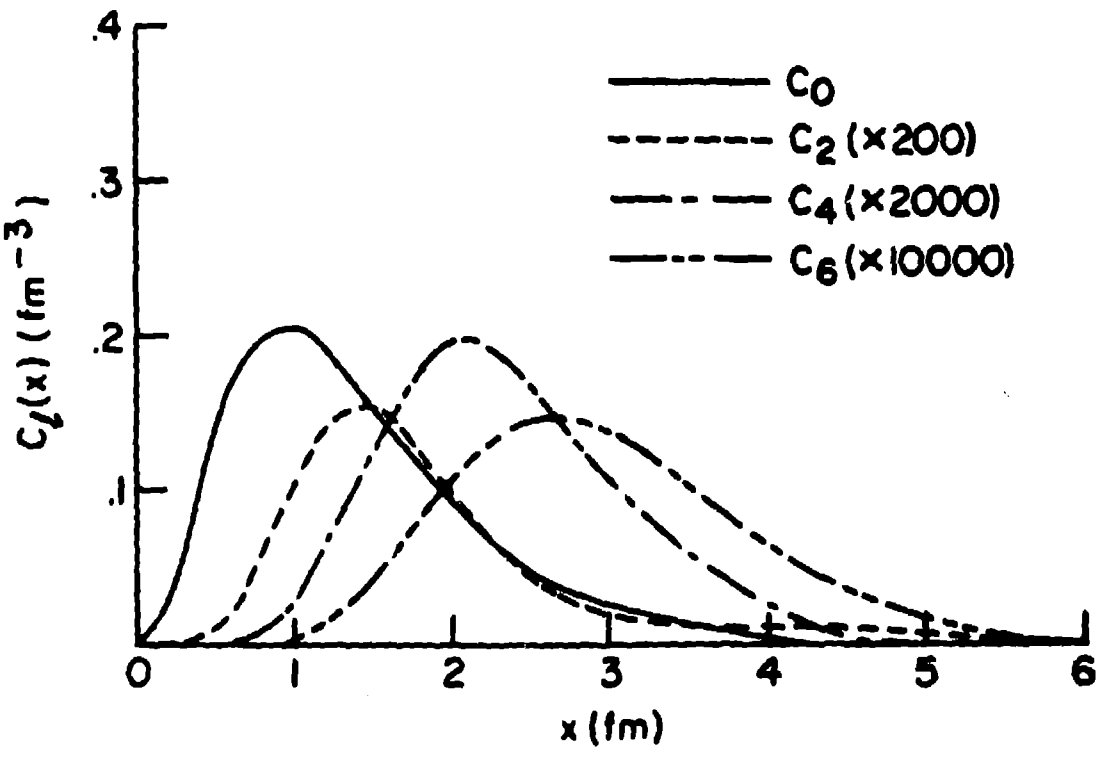
.4
.3
.2
.1
$C_\ell(x)$ (fm^{-3})
C_0
C_2 (×200)
C_4 (×2000)
C_6 (×10000)
0
1
2
3
4
5
6
x (fm)

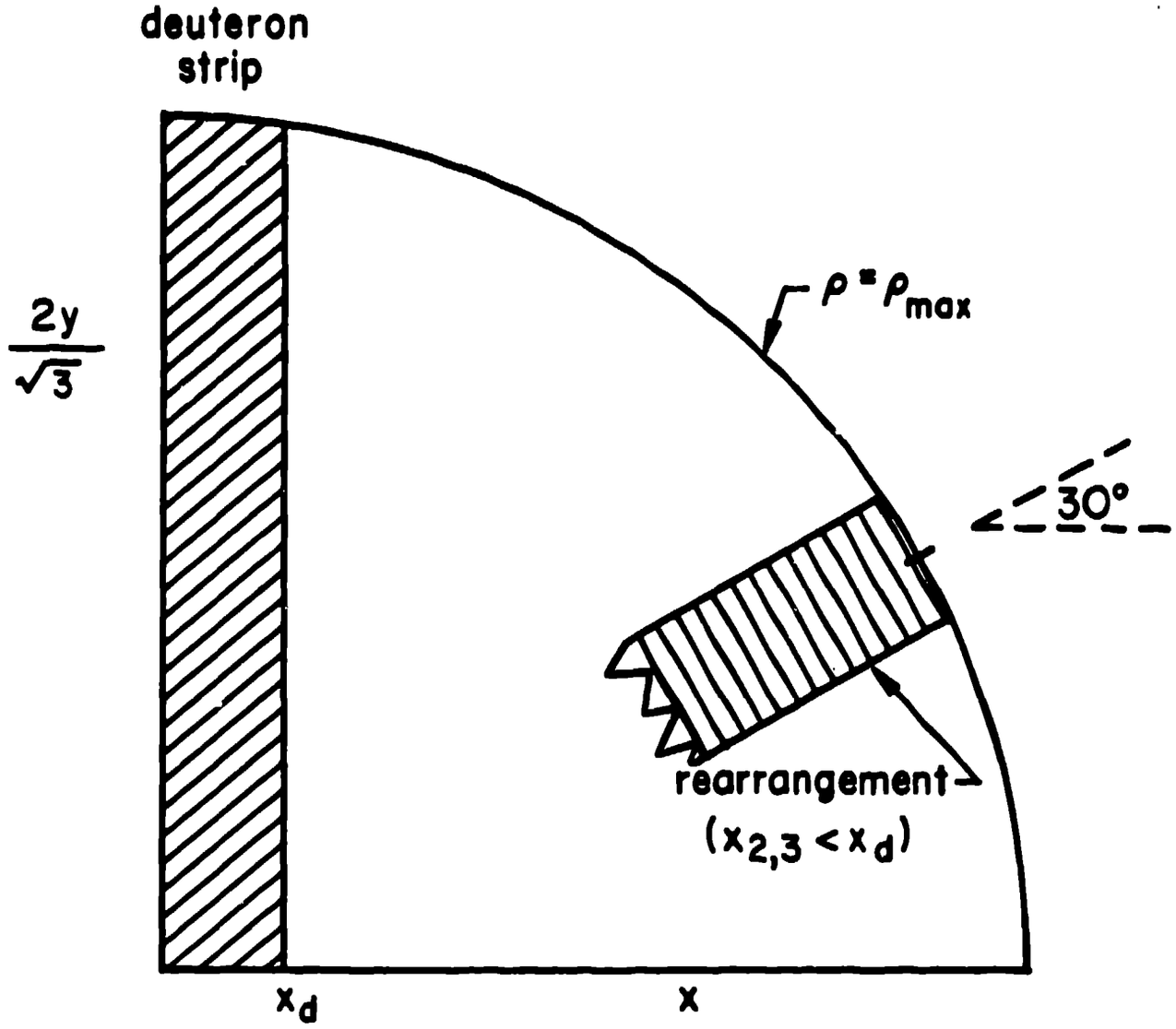

$$x = \rho \cos \theta'$$

$$y = \frac{\sqrt{3}}{2} \rho \sin \theta'$$

ψ_1

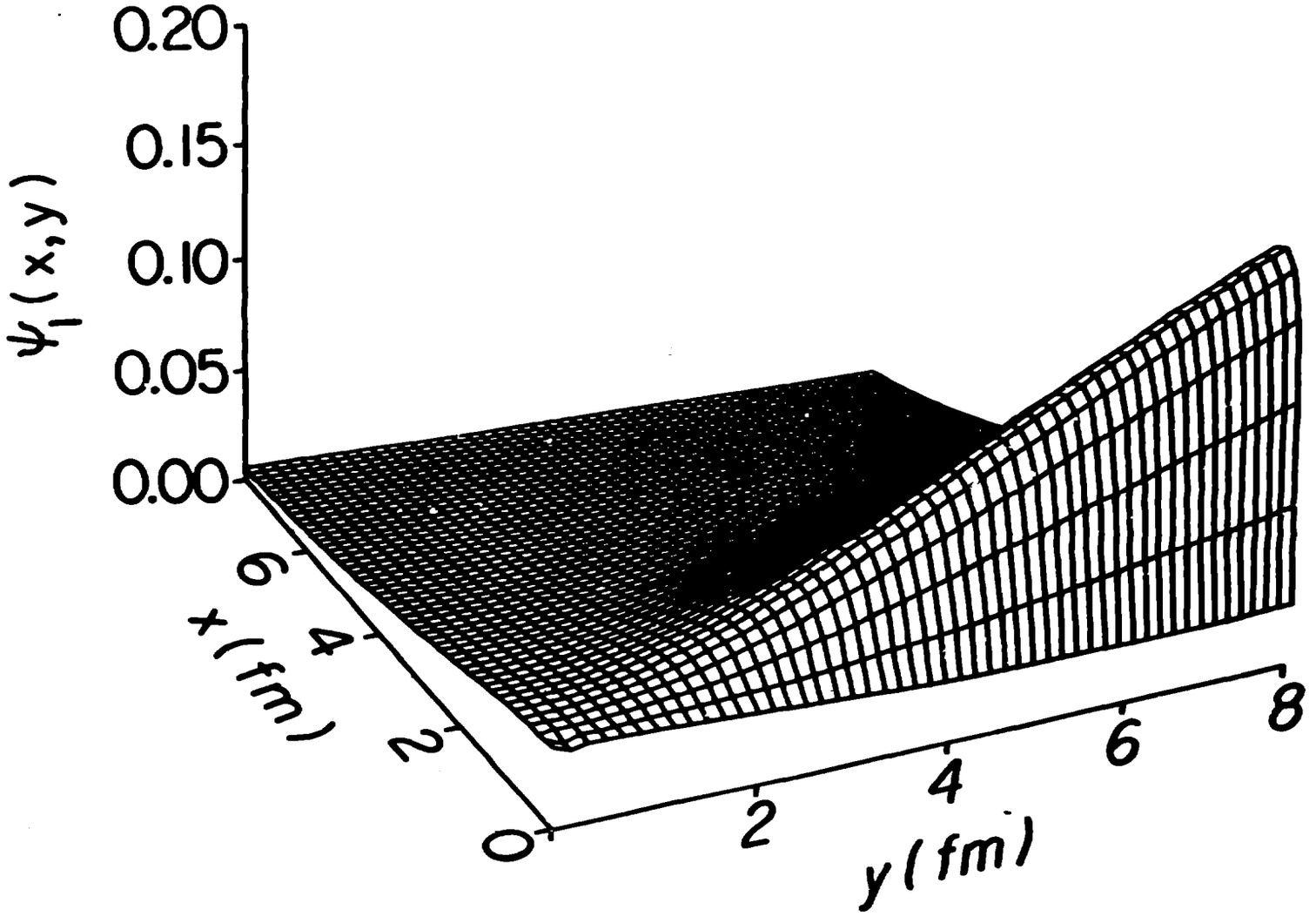

V_3 $\theta = 0°$

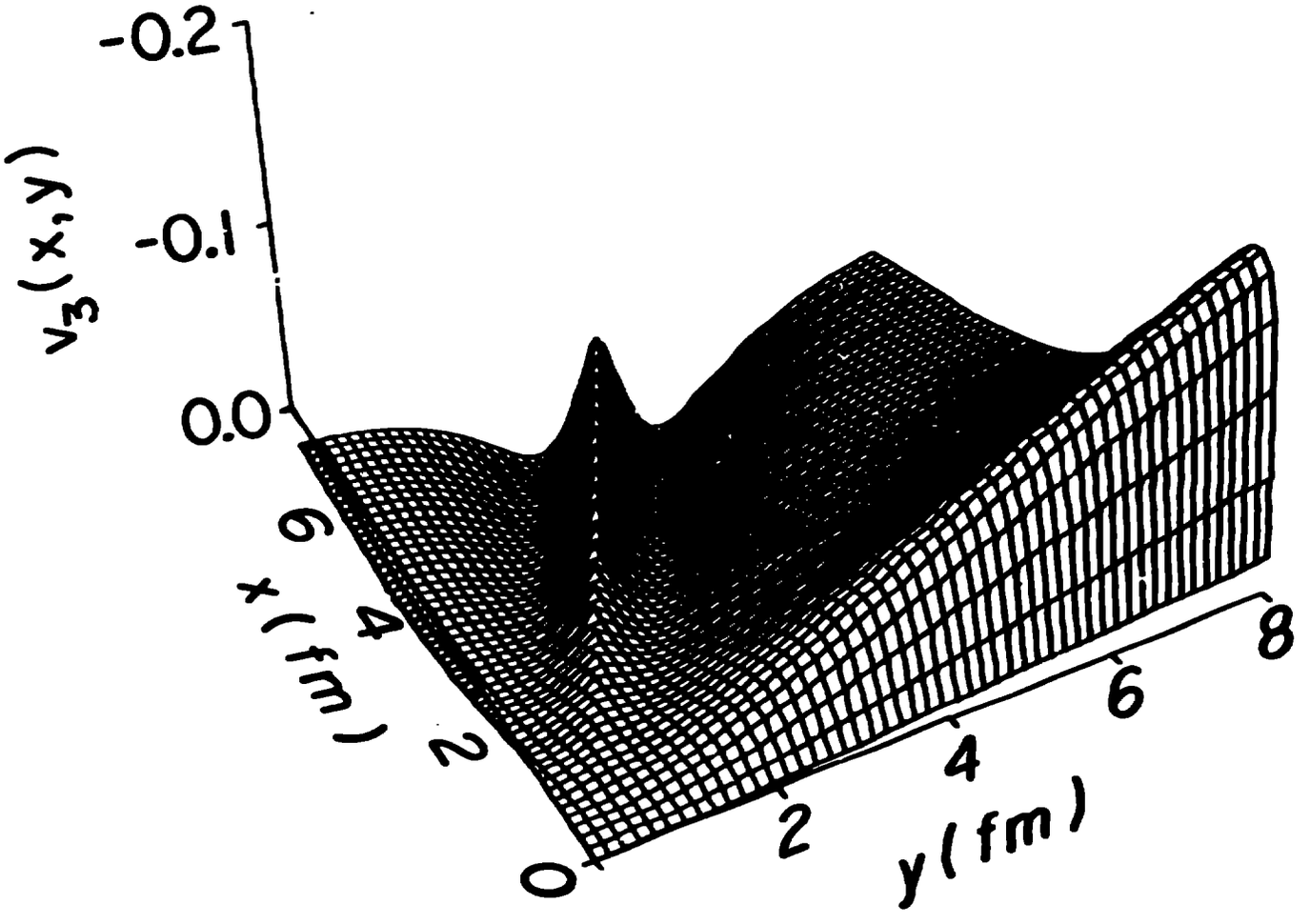

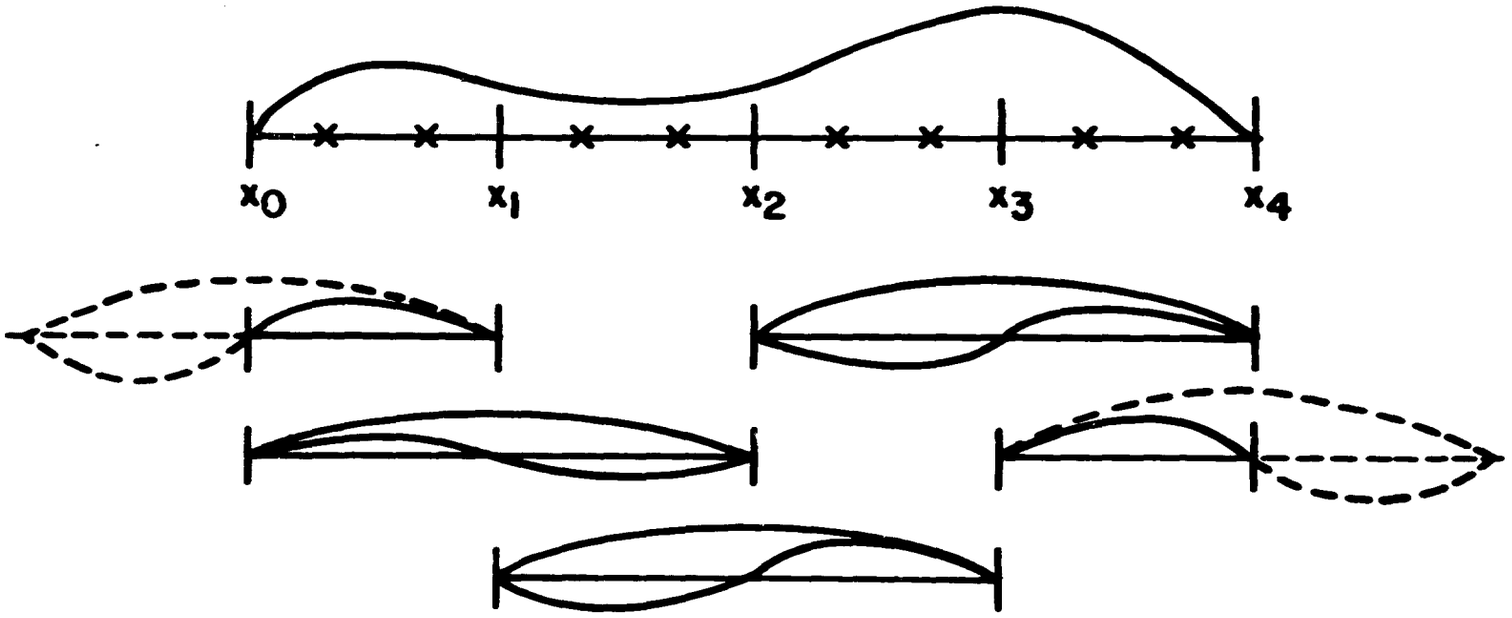
x0
x1
x2
x3
x4

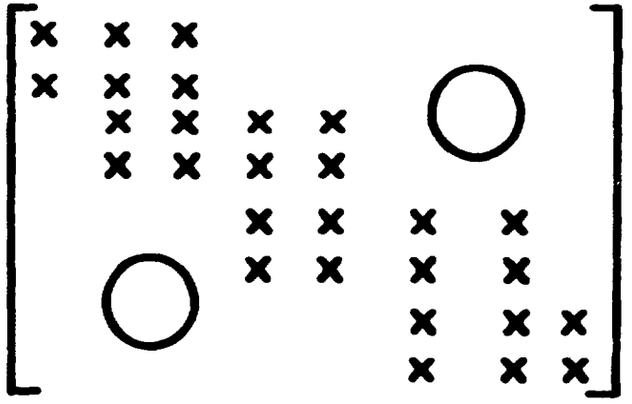

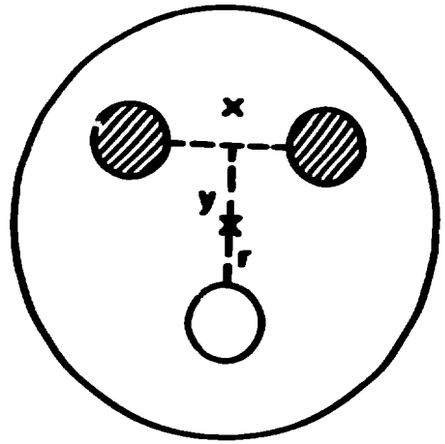

(a)

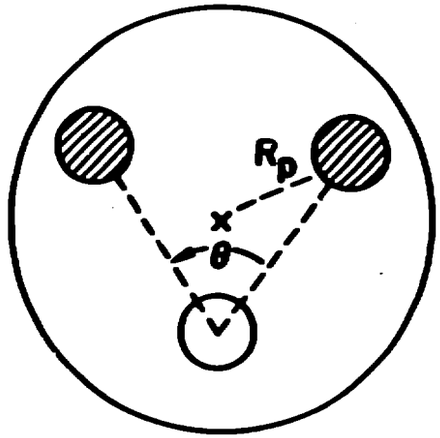

(b)

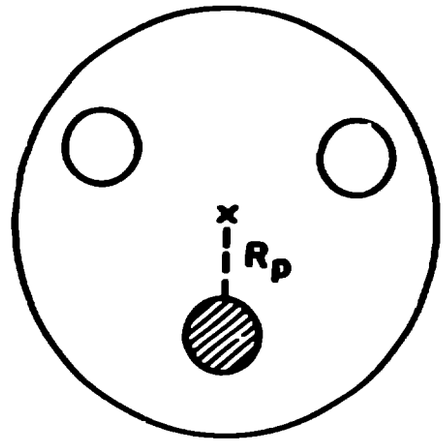

(c)

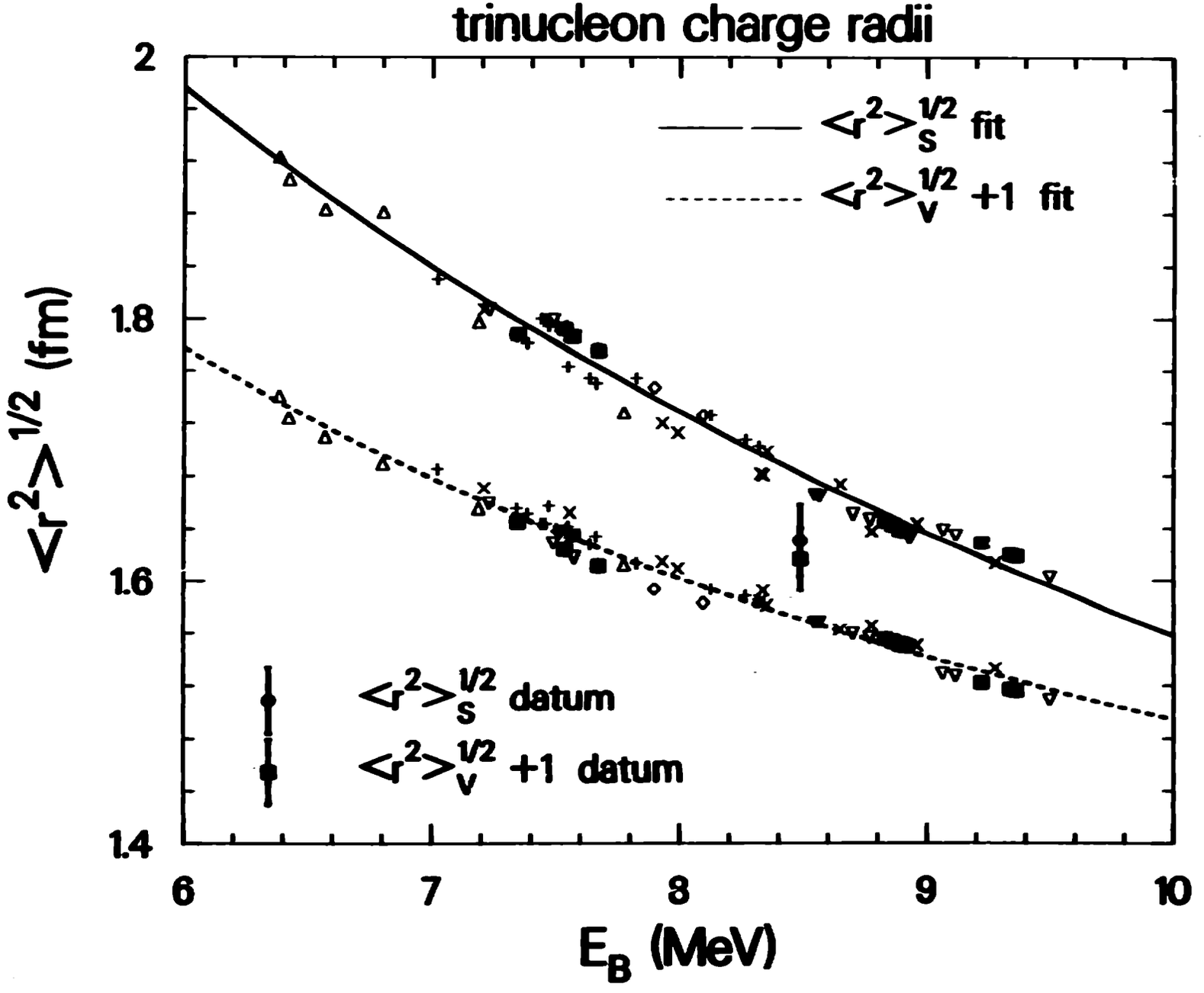
trinucleon charge radii
2
1.8
1.6
1.4
6
7
8
9
10
$\langle r^2 \rangle^{1/2}$ (fm)
E_B (MeV)
$\langle r^2 \rangle_S^{1/2}$ fit
$\langle r^2 \rangle_V^{1/2}$ +1 fit
$\langle r^2 \rangle_S^{1/2}$ datum
$\langle r^2 \rangle_V^{1/2}$ +1 datum

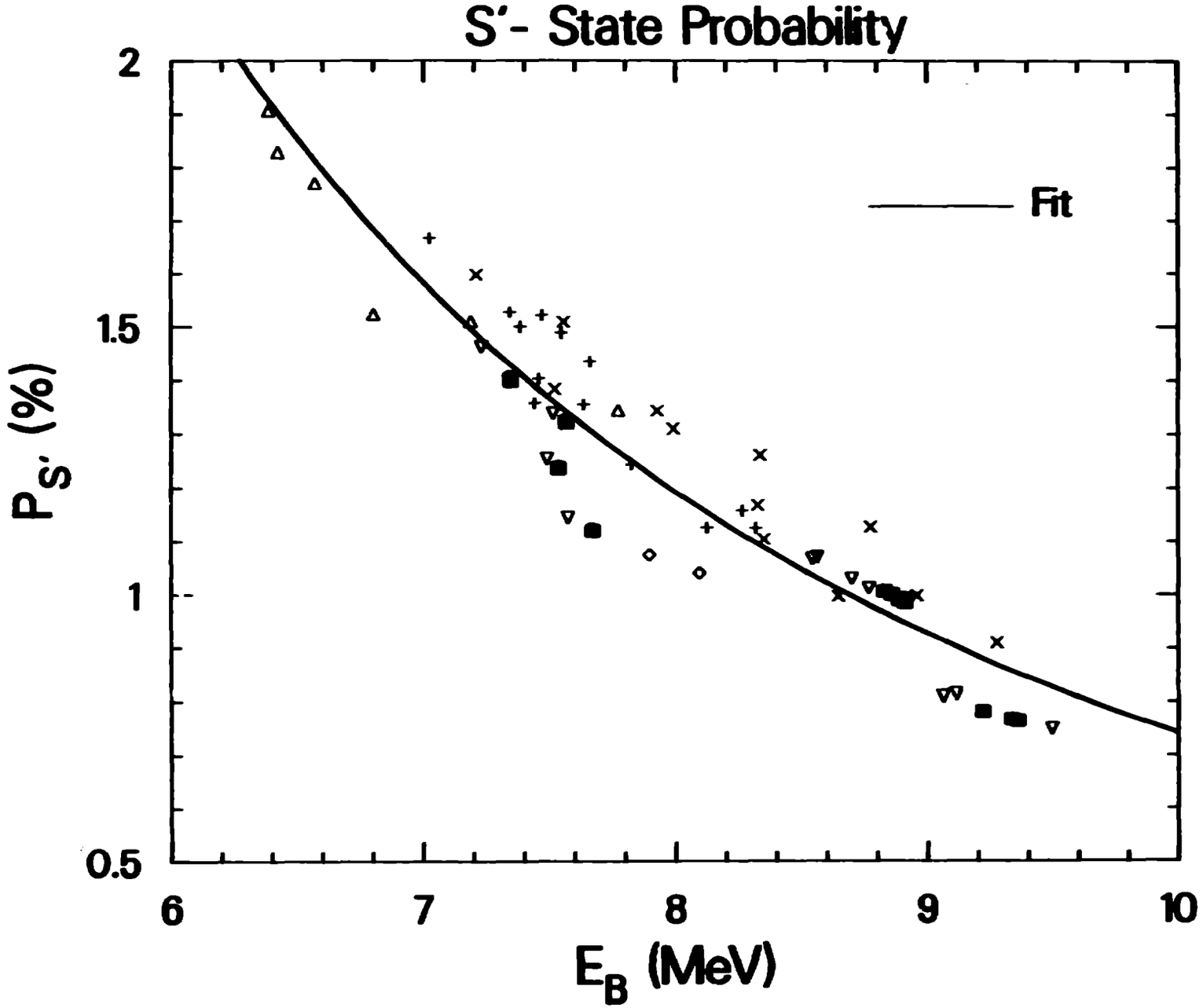
S'- State Probability
2
1.5
1
0.5
$P_{S'}$ (%)
Fit
6
7
8
9
10
E_B (MeV)

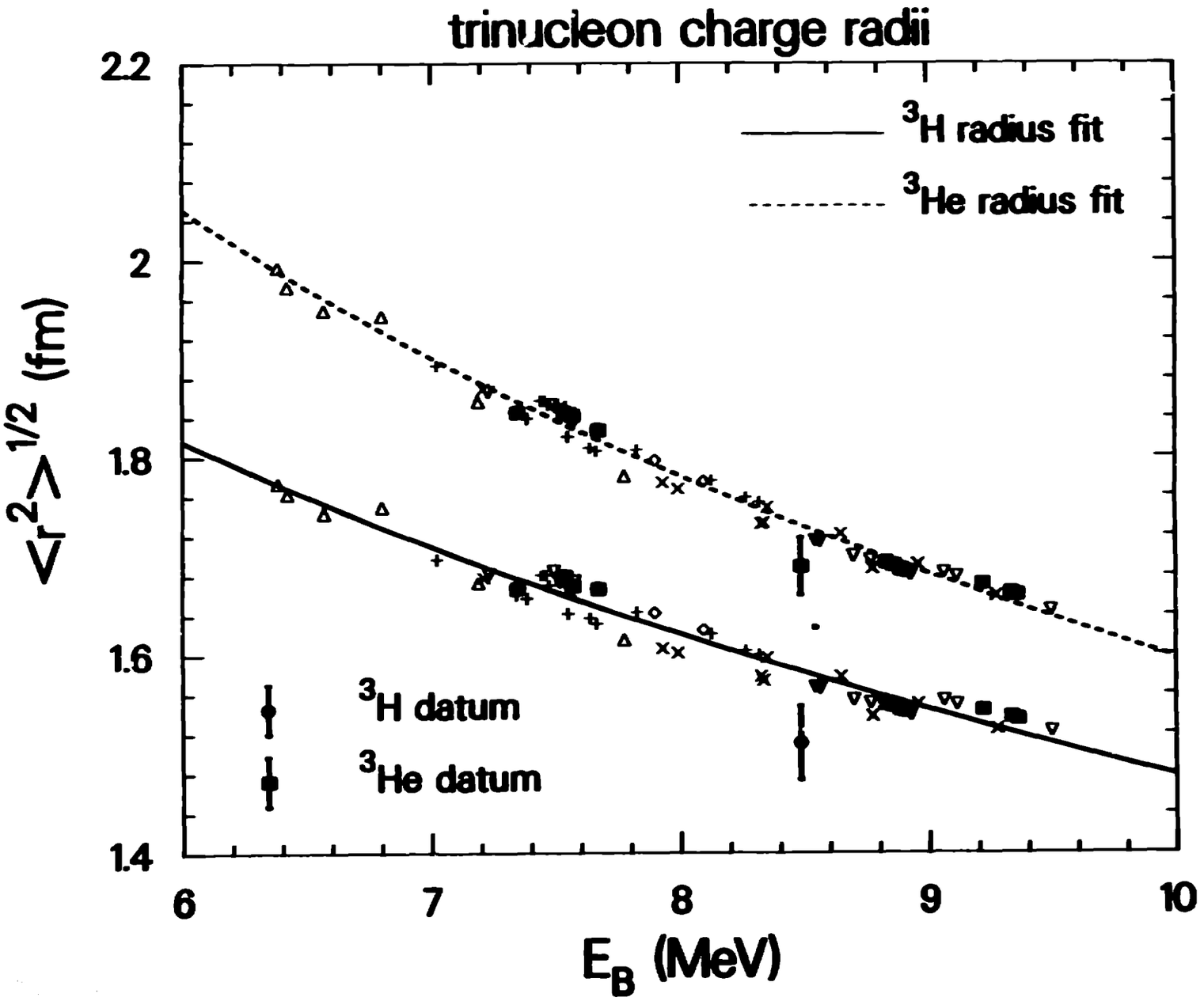
trinucleon charge radii
2.2
2
1.8
1.6
1.4
6
7
8
9
10
$\langle r^2 \rangle^{1/2}$ (fm)
E_B (MeV)
^{3}H radius fit
^{3}He radius fit
^{3}H datum
^{3}He datum

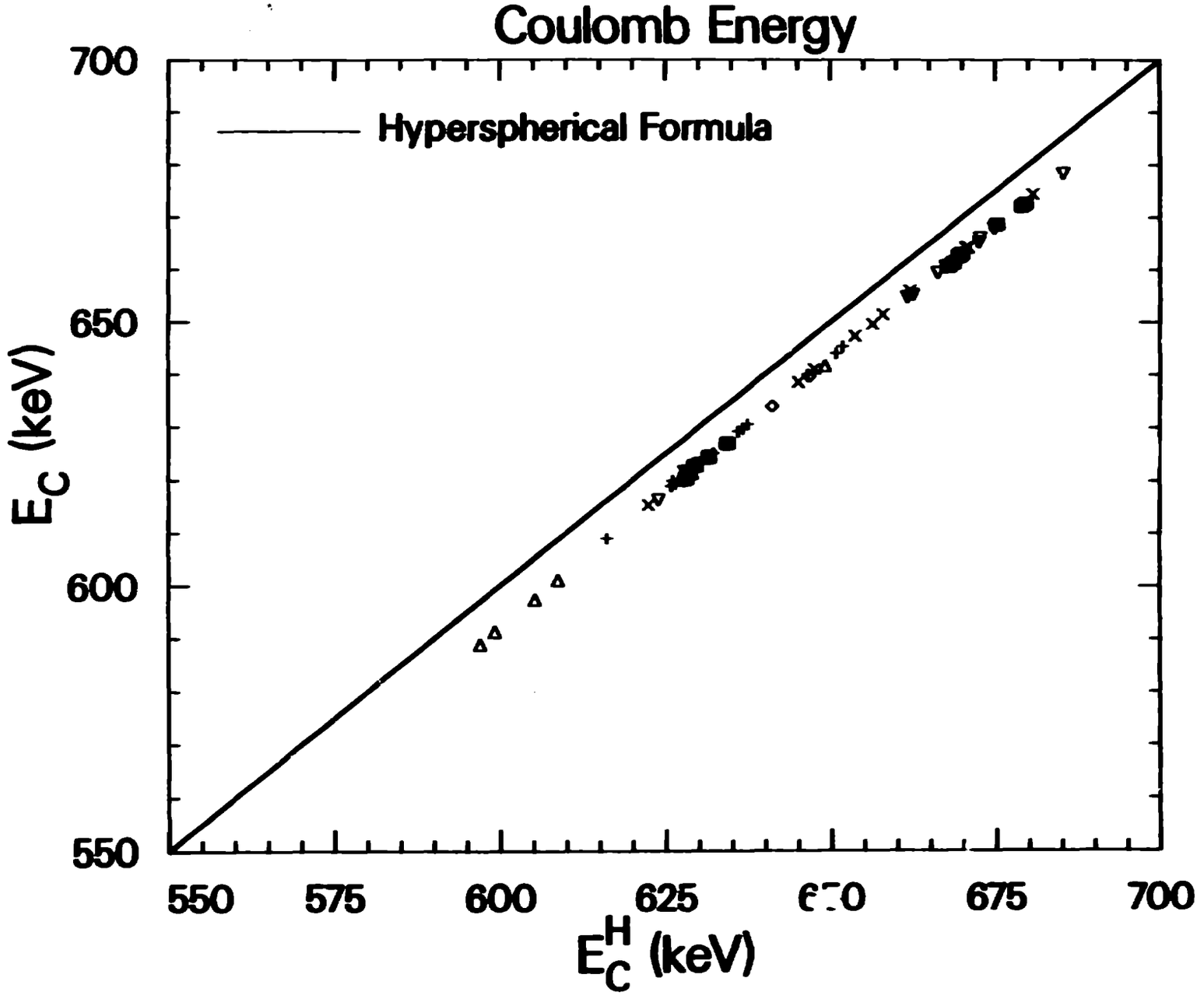
Coulomb Energy
Hyperspherical Formula
700
650
600
550
E_C (keV)
550
575
600
625
675
700
E_C^H (keV)

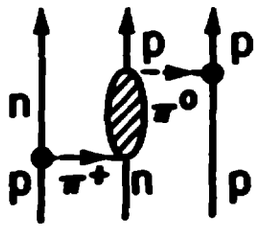

(a)

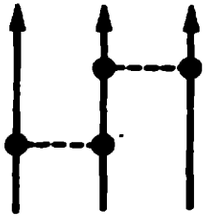

(b)

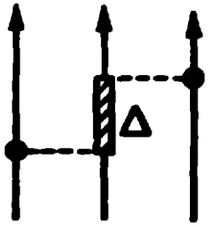

(c)

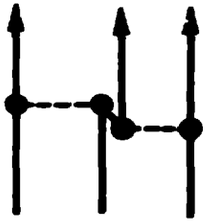

(d)

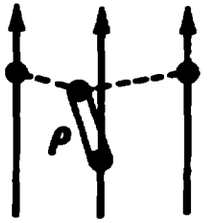

(e)

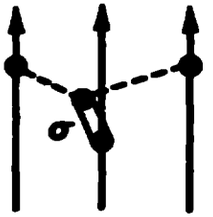

(f)

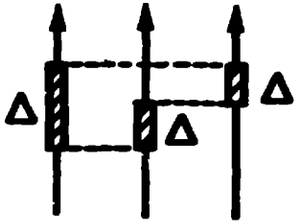

(g)

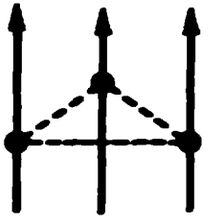

(h)

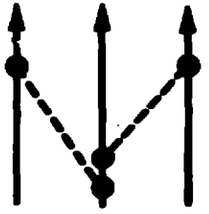

(i)

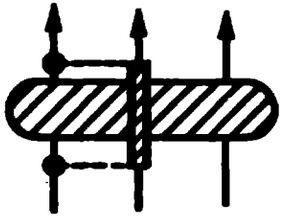

(j)

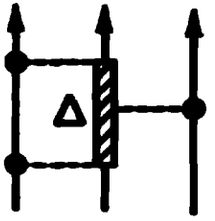

(k)

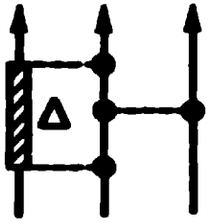

(ℓ)

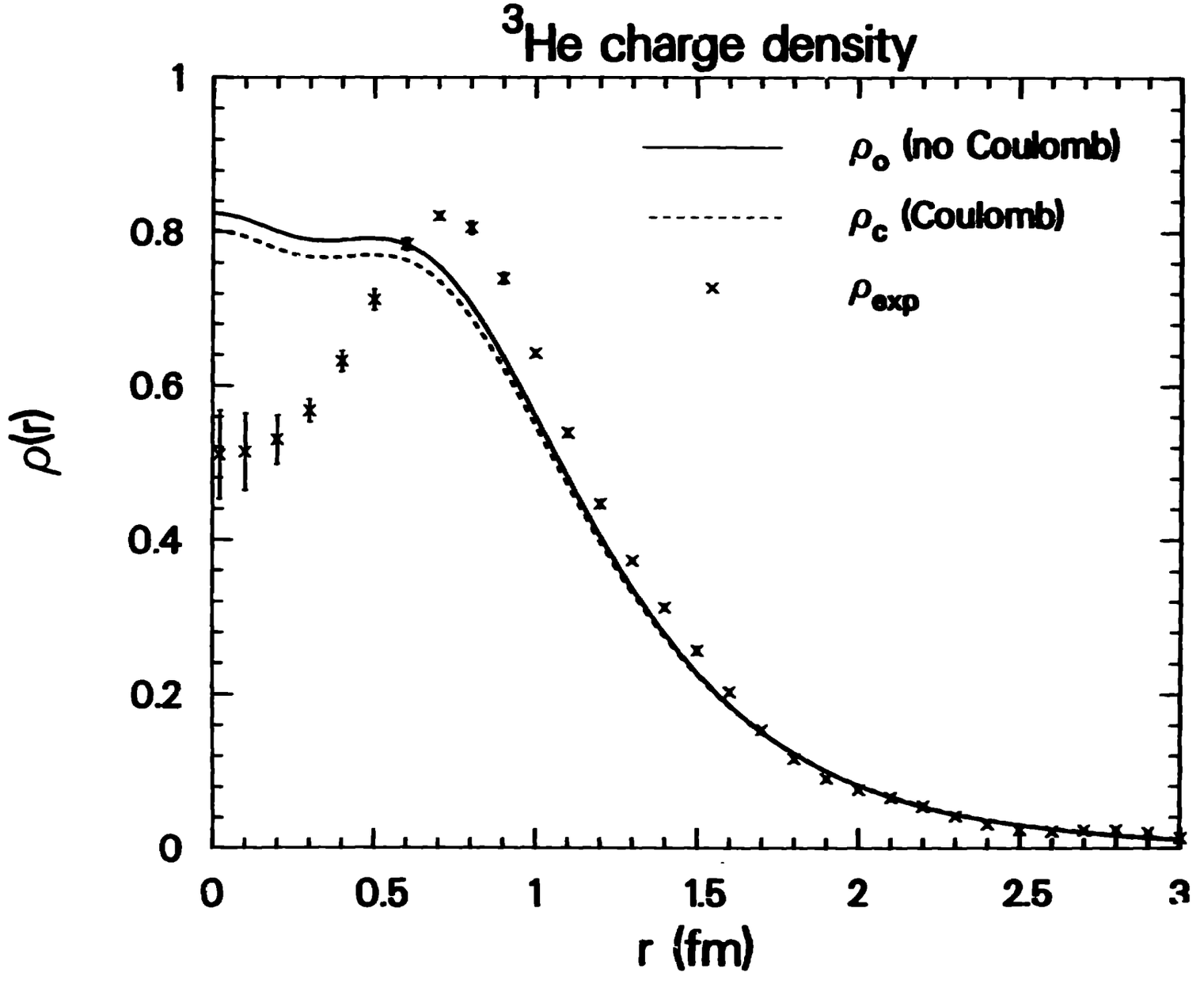
^{3}He charge density
ρ_o (no Coulomb)
ρ_c (Coulomb)
ρ_{exp}
$\rho(r)$
r (fm)
0
0.2
0.4
0.6
0.8
1
0
0.5
1
1.5
2
2.5
3

u

RSC5

$\theta = 0°$

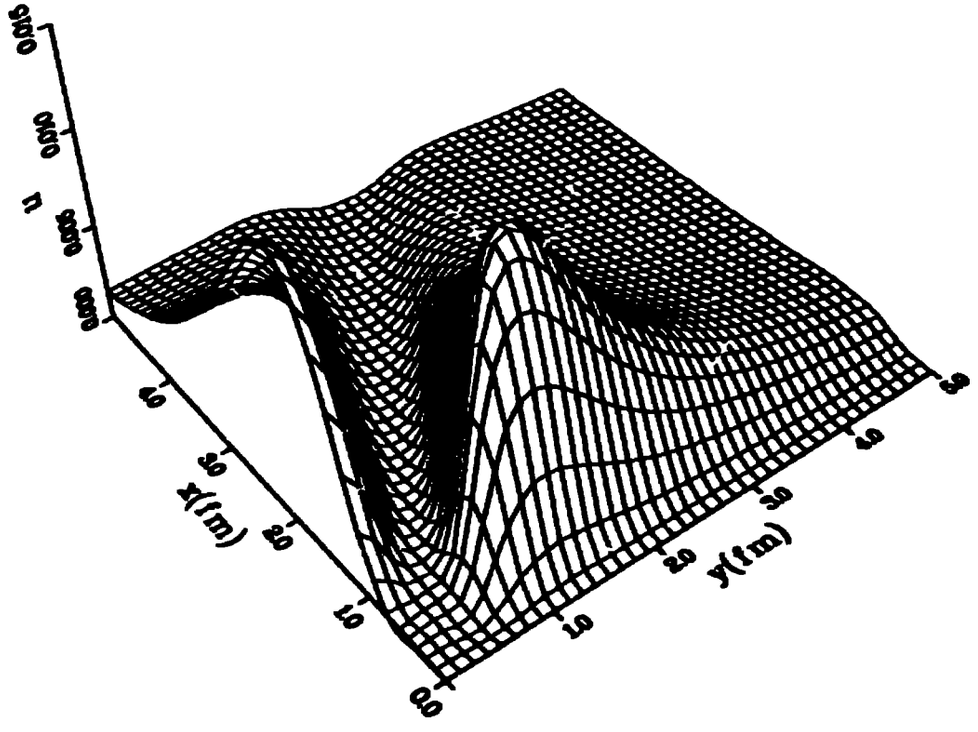

ψ_1^S

RSC5
θ=90°

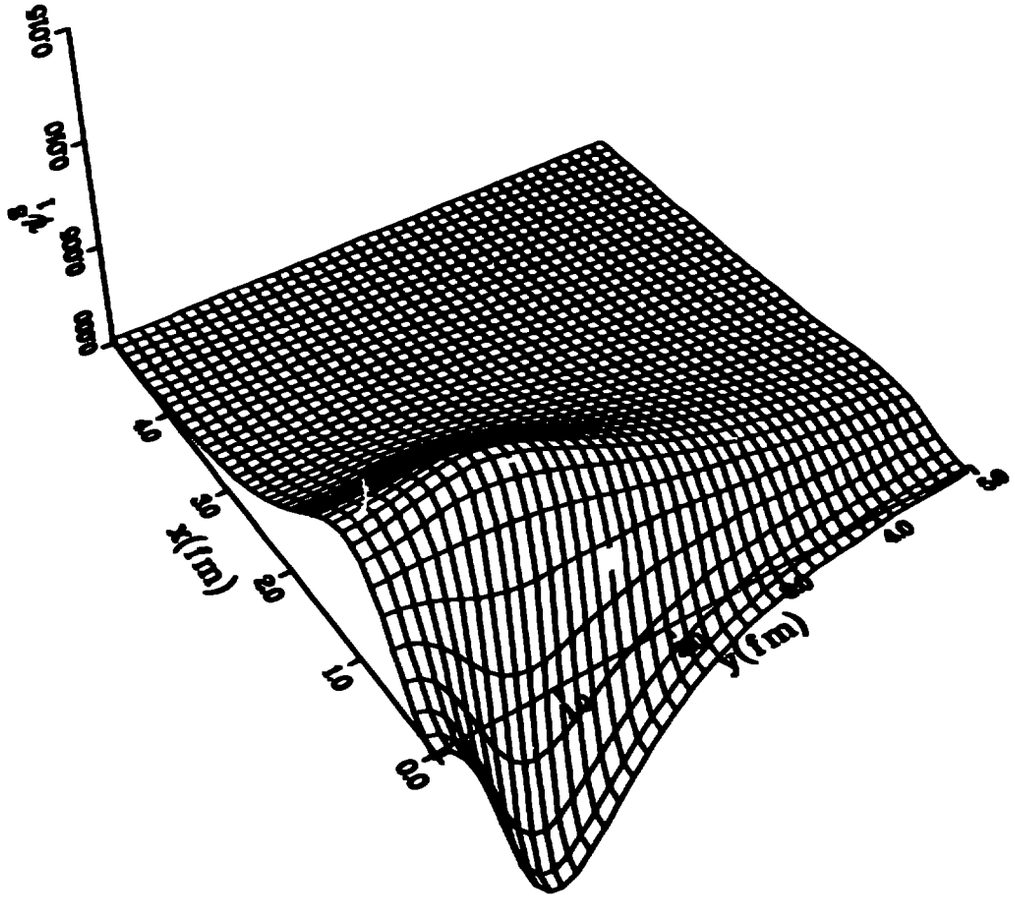

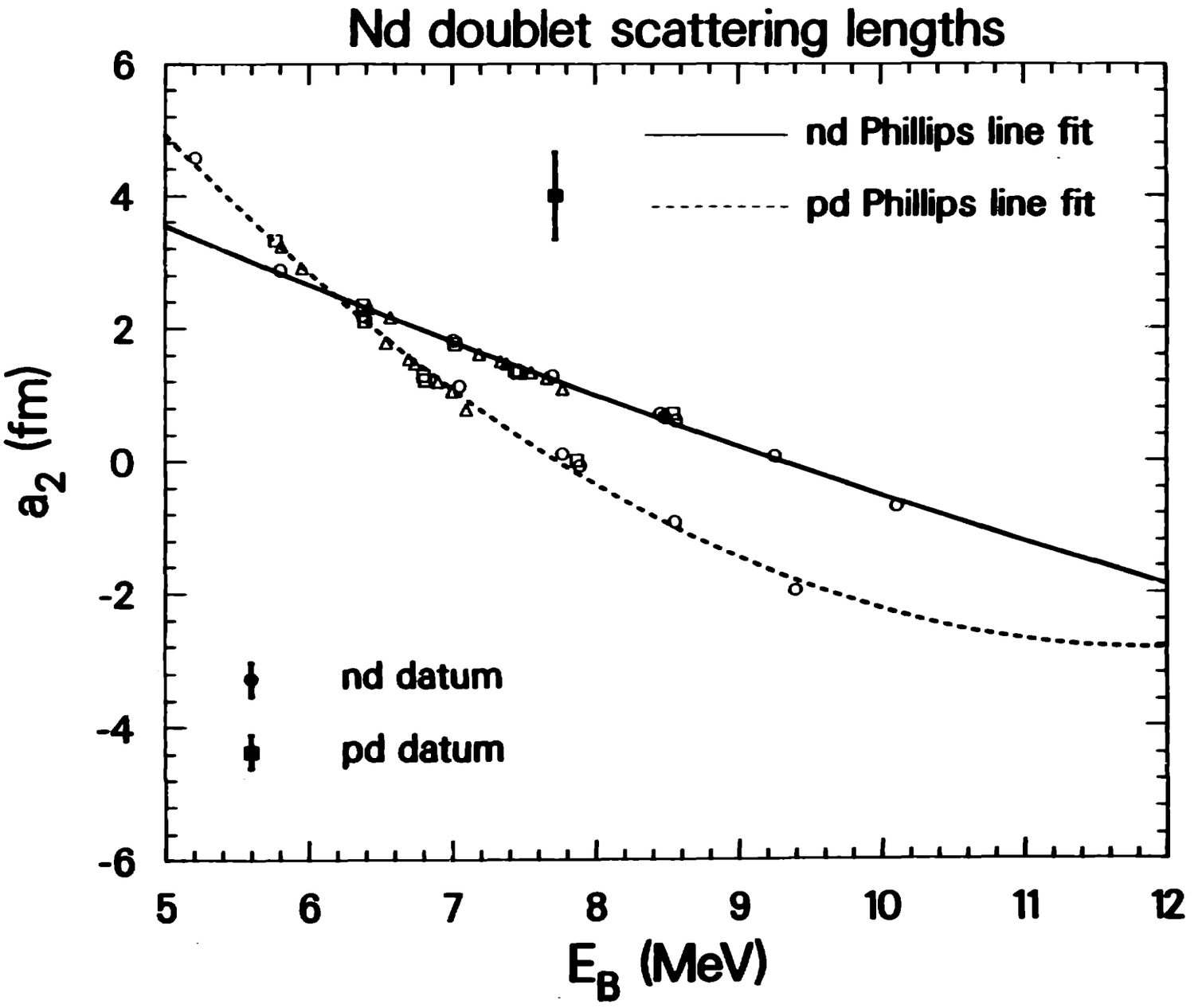
Nd doublet scattering lengths
nd Phillips line fit
pd Phillips line fit
nd datum
pd datum
a_2 (fm)
E_B (MeV)
6
4
2
0
-2
-4
-6
5
6
7
8
9
10
11
12

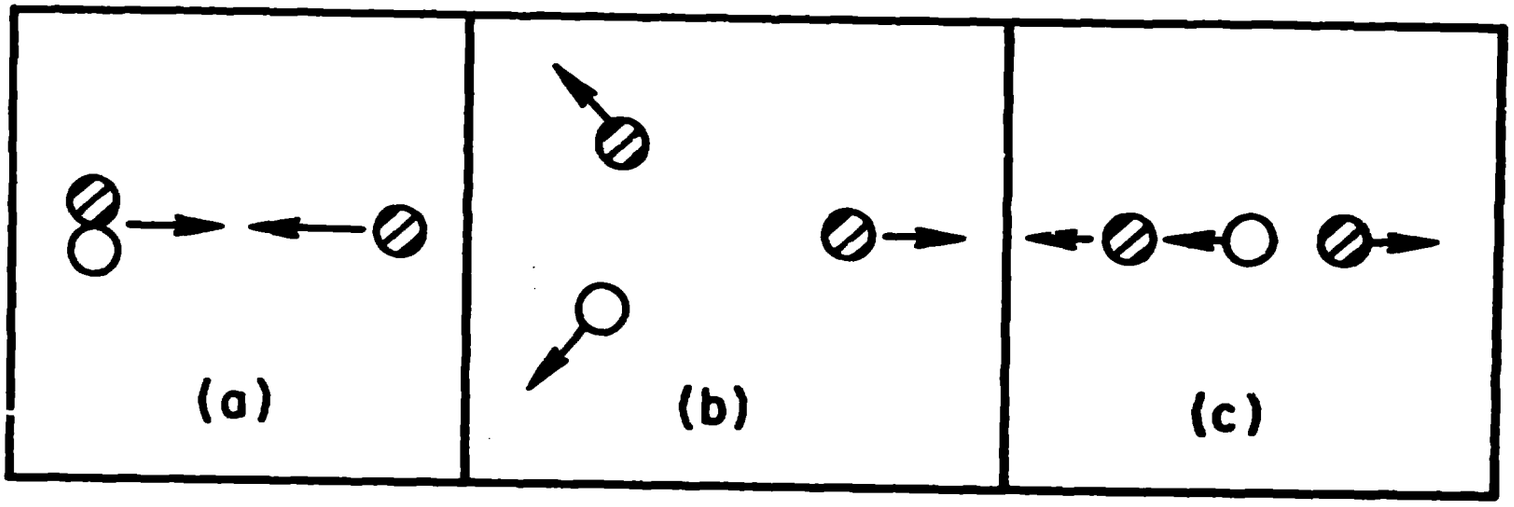
(a)
(b)
(c)

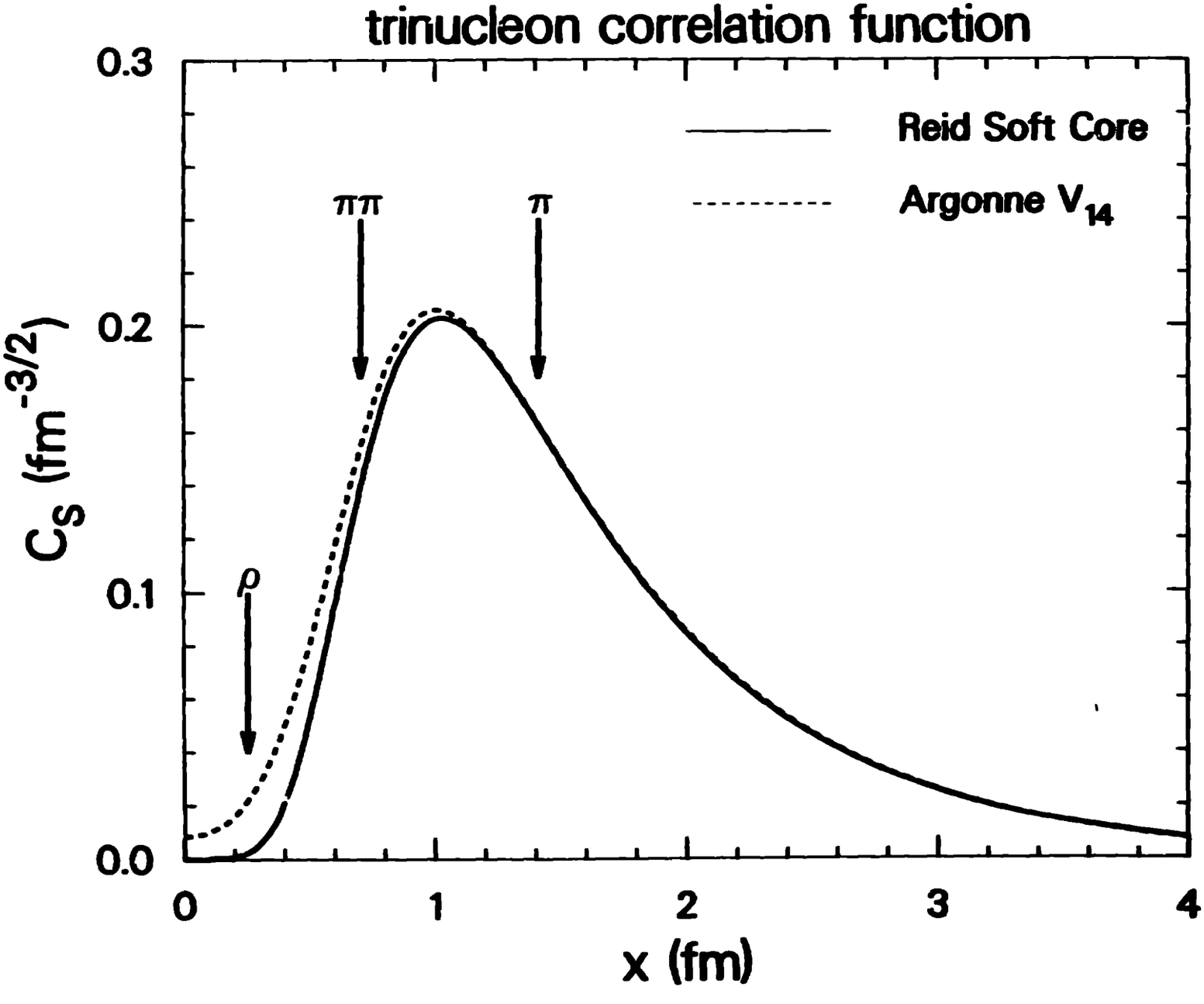
trinucleon correlation function
0.3
0.2
0.1
0.0
C_S (fm$^{-3/2}$)
Reid Soft Core
Argonne V_{14}
$\pi\pi$
π
ρ
0
1
2
3
4
x (fm)

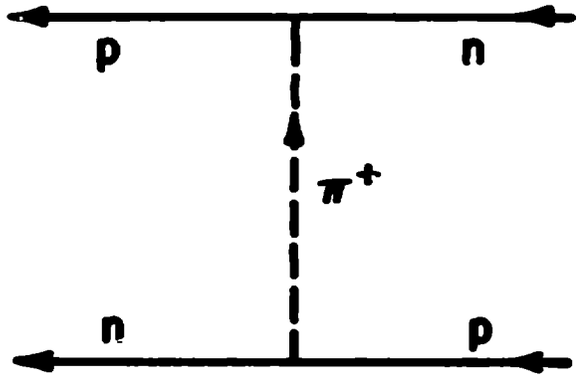

(a)

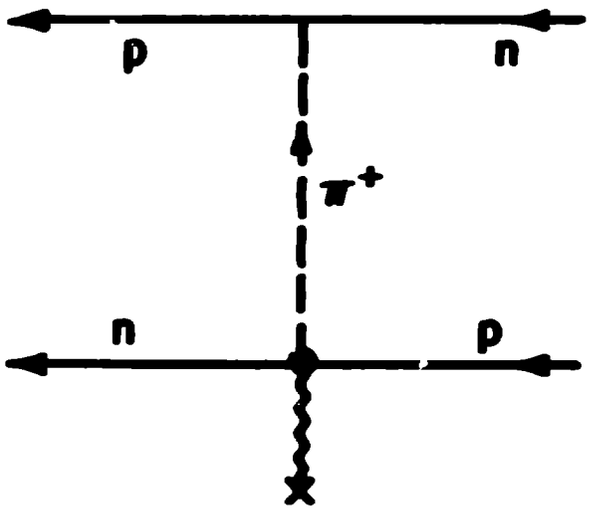

(b)

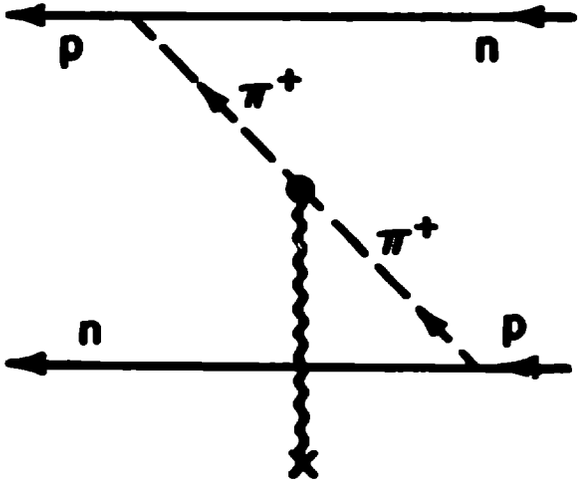

(c)

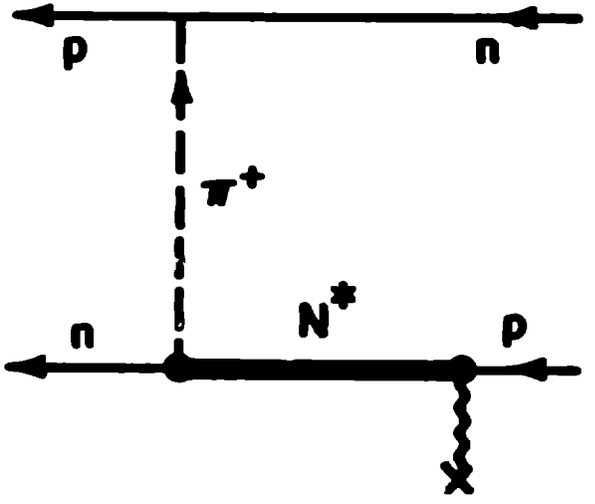

(d)

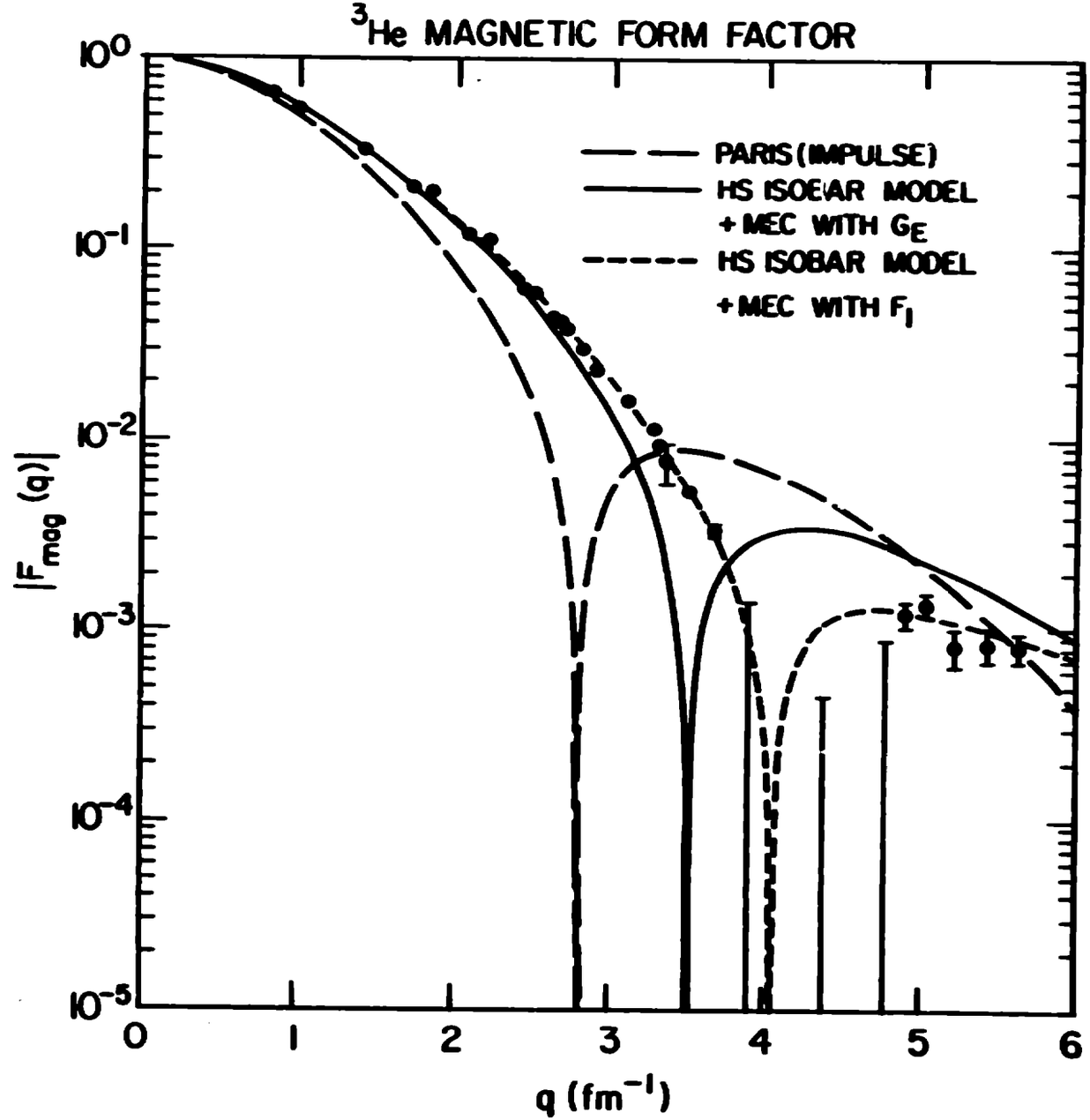
^{3}He MAGNETIC FORM FACTOR
PARIS (IMPULSE)
HS ISOBAR MODEL
+ MEC WITH G_E
HS ISOBAR MODEL
+ MEC WITH F_1
$|F_{mag}(q)|$
10^0
10^{-1}
10^{-2}
10^{-3}
10^{-4}
10^{-5}
0
1
2
3
4
5
6
q (fm^{-1})

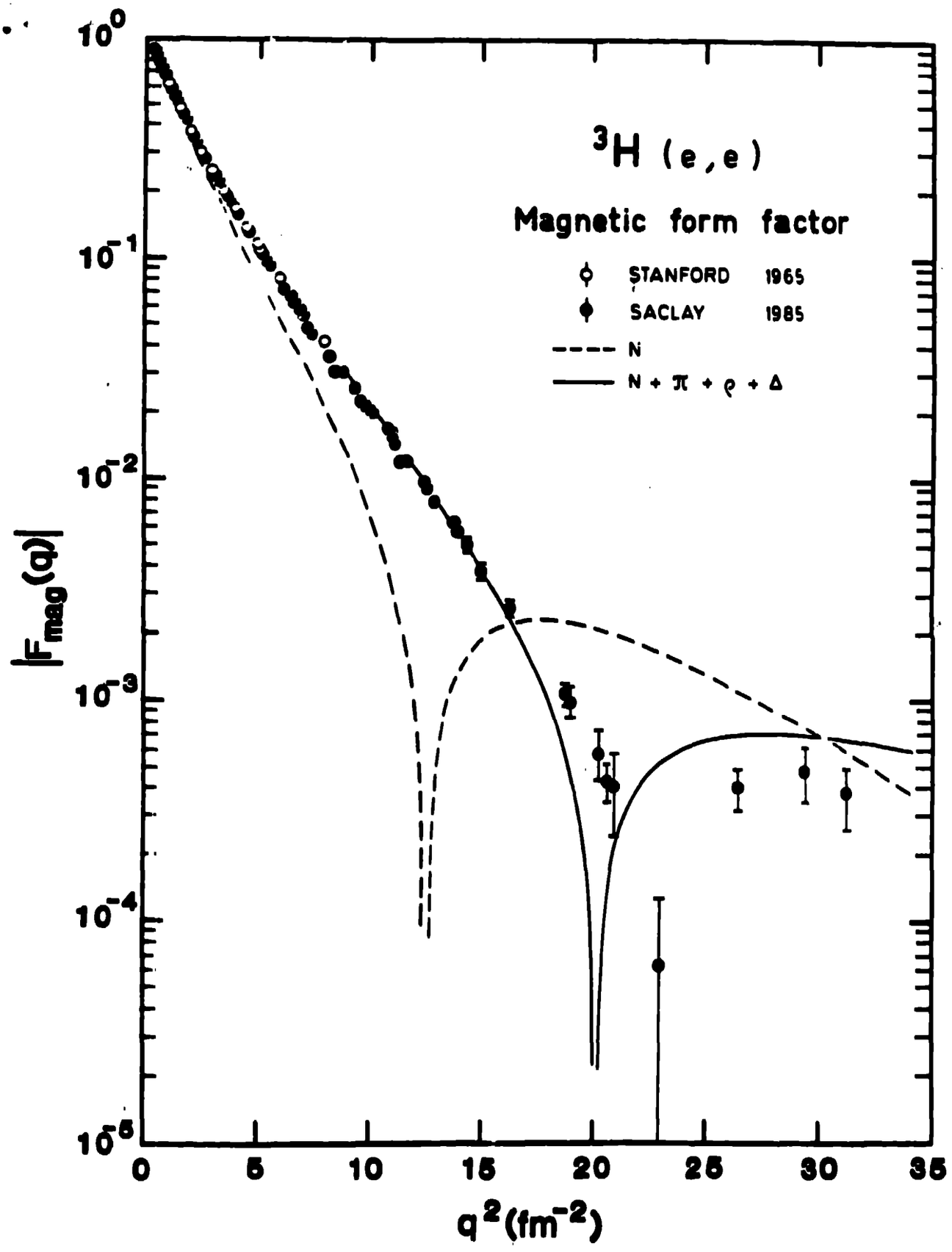
^3H (e,e)
Magnetic form factor
STANFORD 1965
SACLAY 1985
N
N + π + ρ + Δ
$|F_{mag}(q)|$
$q^2(fm^{-2})$
10^0
10^{-1}
10^{-2}
10^{-3}
10^{-4}
10^{-5}
0
5
10
15
20
25
30
35

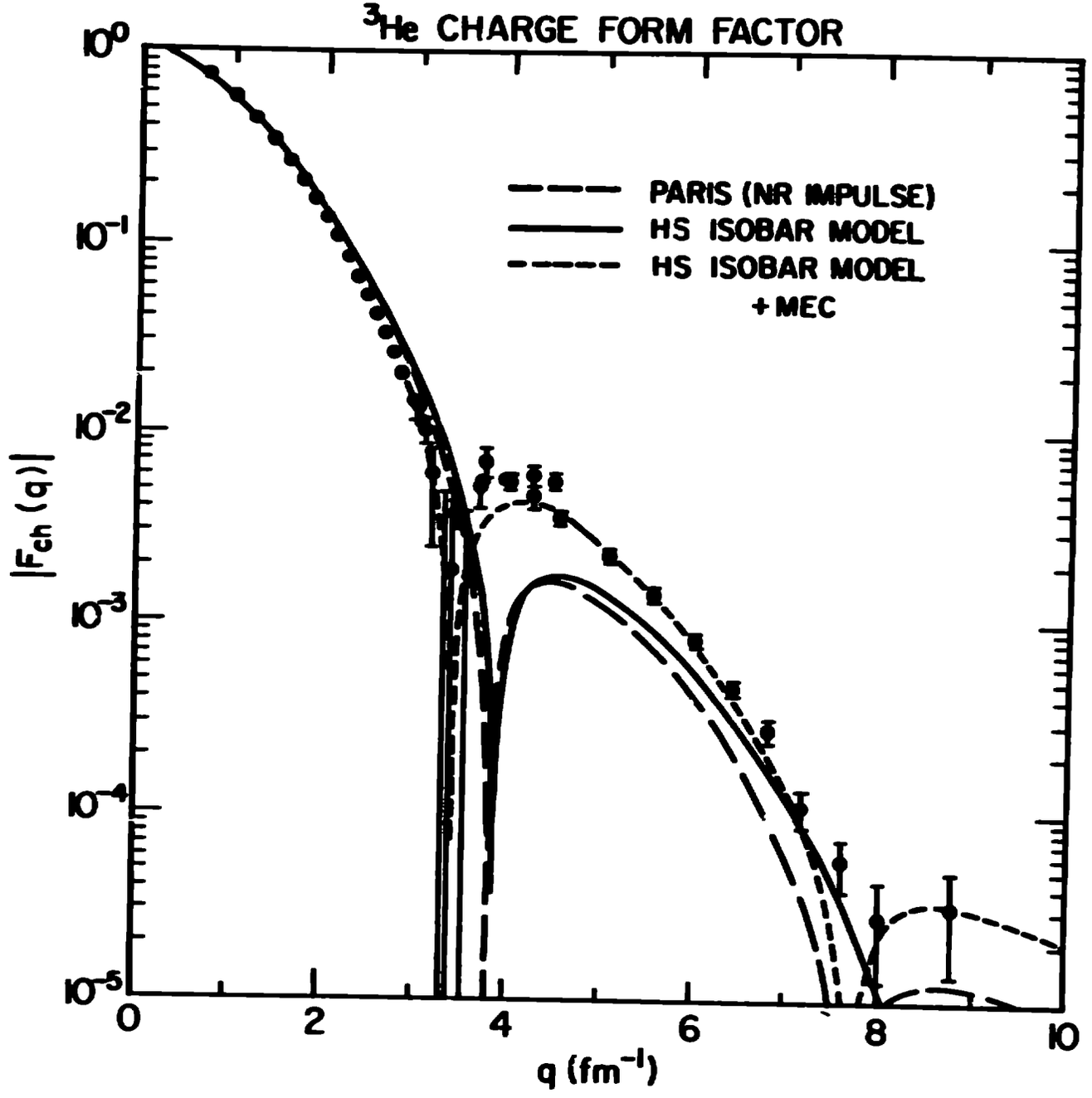
^{3}He CHARGE FORM FACTOR
PARIS (NR IMPULSE)
HS ISOBAR MODEL
HS ISOBAR MODEL
+MEC
$|F_{ch}(q)|$
10^0
10^{-1}
10^{-2}
10^{-3}
10^{-4}
10^{-5}
0
2
4
6
8
10
q (fm^{-1})

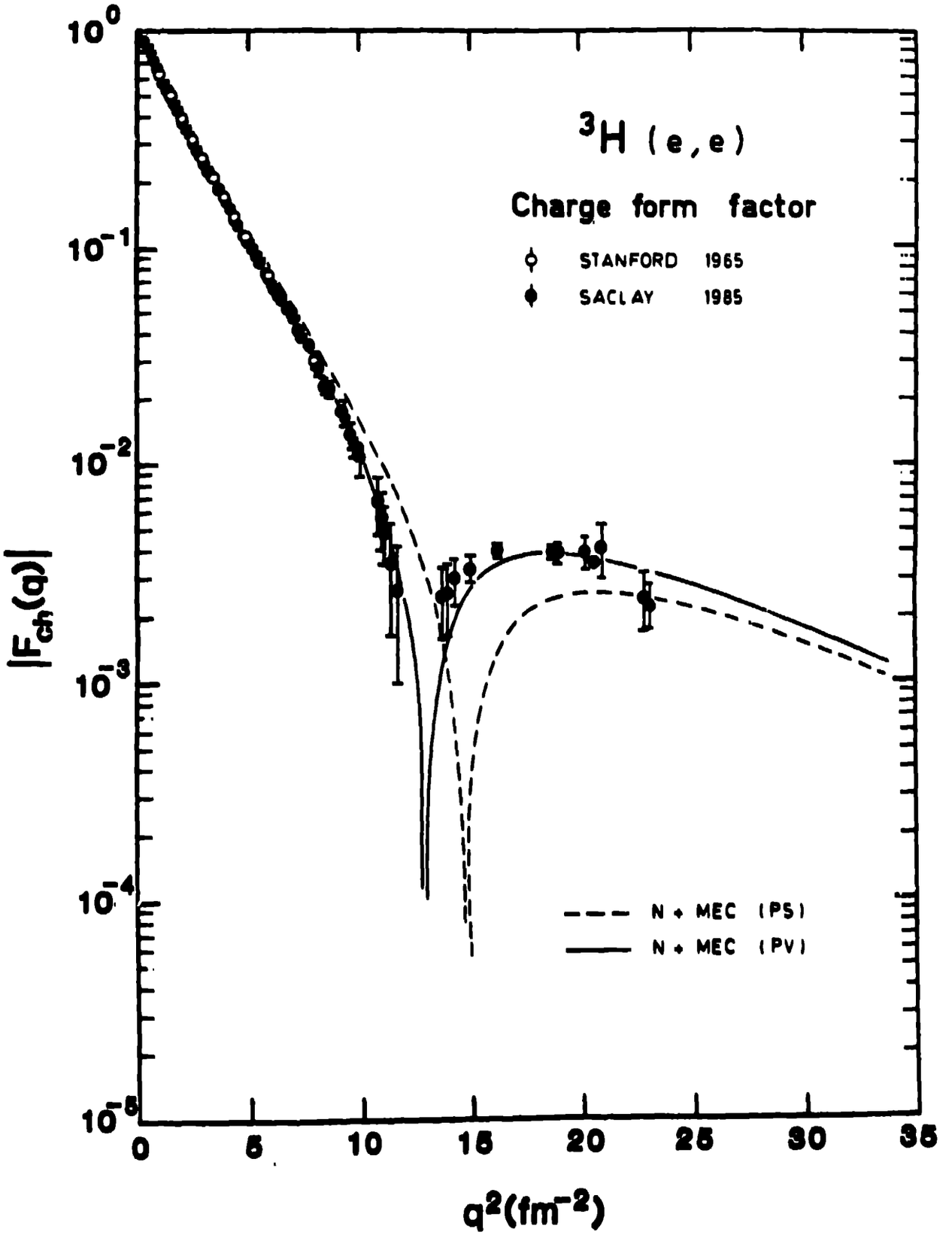
^3H (e,e)
Charge form factor
STANFORD 1965
SACLAY 1985
N + MEC (PS)
N + MEC (PV)
$|F_{ch}(q)|$
$q^2(fm^{-2})$
10^0
10^{-1}
10^{-2}
10^{-3}
10^{-4}
10^{-5}
0
5
10
15
20
25
30
35